RESEARCH AND DEVELOPMENT TECHNICAL REPORT
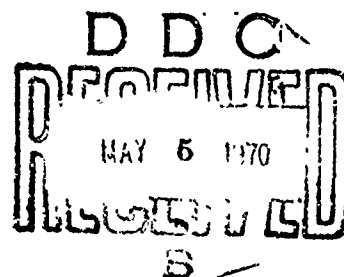## ECOM-3246

RADAR RESPONSE OF LONG WIRES

By

F. SCHWERING

MARCH 1970

D D C

DISTRIBUTION STATEMENT (1)

This document has been approved for public release and sale, its distribution is unlimited.

ECOM

UNITED STATES ARMY ELECTRONICS COMMAND · FORT MONMOUTH, N.J.

RESEARCH AND DEVELOPMENT TECHNICAL REPORT

ECOM - 3246

RADAR RESPONSE OF LONG WIRES

by

F. Schwering

Institute for Exploratory Research

U. S. Army Electronics Command

Fort Monmouth, New Jersey

MARCH 1970
DA TASK No. 1TO 61102 B31A 01 45

U. S. ARMY ELECTRONICS COMMAND
FORT MONMOUTH, NEW JERSEY

ABSTRACT

Scatter field and radar response of an infinitely long straight metallic wire are derived assuming that the wire is illuminated by an antenna radiating a Gaussian beam of narrow beam width. The scatter field has essentially the same distribution in any plane through the wire axis; it varies from plane to plane by only an amplitude factor. The radar response is at a maximum for vertical incidence - when the beam axis intersects the wire axis at right angles - and decreases exponentially with increasing inclination of the beam axis against this direction. No side lobes are obtained for Gaussian illumination, at least not in the interesting range of small angular deviations from vertical incidence where the radar response has appreciable values. Two cases can be distinguished: (1) the wire crosses the Fresnel region of the antenna and (2) the wire is situated in the antenna far zone. In the former case, the theory is limited to wire radii not exceeding the beam radius at the antenna; in the latter case, arbitrary wire radii are admissible. If the wire is located in the far field region of the antenna, the expression derived for the radar response can be generalized so that it applies to any antenna characteristic. The generalized expression shows that a radar cross section can be assigned to the wire even though it has been assumed to be infinitely long; this radar cross section increases linearly with distance between antenna and wire.

CONTENTS

FIGURES

APPENDICES

iv

RADAR RESPONSE OF LONG WIRES

1. INTRODUCTION

Helicopters flying at low altitudes must avoid collision with natural and man-made obstructions. The visibility of these obstacles depends, apart from weather conditions, on their geometrical configuration. The geometrical configuration of thin wires with long suspension lengths is particularly inconspicuous, and the question arises whether such wires can be detected at safe distances by the helicopter radar system.

To obtain quantitative information on this problem the scatter properties of straight metallic wires are derived in this paper; the assumption is made that an antenna emitting a time-harmonic beam with a narrow Gaussian radiation characteristic is the source of excitation. The wire is assumed to have circular cross-section and to be long compared to the antenna-beam diameter at the location of the wire. The scatter field produced by diffraction of the incident beam at the wire is derived, and the fraction of the radiated power which in this scatter field is returned to and received by the antenna is calculated.

By means of the reciprocity theorem, a general formula can be determined for the ratio of received and transmitted antenna power. This formula holds for any scatter object and any antenna characteristic. When applied to a straight metallic wire illuminated by a Gaussian antenna, this formula leads to an expression containing triple integrals. A rigorous evaluation of these integrals is mathematically difficult, but with appropriate approximations closed form solutions are obtained for the radar response. The approximations are based on the assumption that the beam width of the incident beam is in the order of 1°.

Two cases can be distinguished, that the wire crosses the Fresnel region[*] of the antenna and that the wire is situated in the far field region of the antenna. The approximations made in the former case limit the applicability of the results to angles of the beam axis against the normal to the wire axis of up to ~15°. This restriction, however, is of no practical consequence as the backscatter power received by the antenna decreases very rapidly as the beam axis is turned away from the direction of vertical incidence. There may be side lobes at larger angles, but the formulas show that if they should exist, their level would be very low.

If the wire is situated in the far field region of the antenna, a general expression for the received backscatter power which holds for any antenna characteristic can be derived. The Gaussian antenna in this case serves only as a specific example. Similar to the case that the wire is within the Fresnel region, the radar response for a Gaussian antenna does not contain side lobes; it decreases exponentially as the beam axis is turned away from the direction of vertical incidence.

Diffraction by straight metallic wires (as well as by dielectric or dielectric-coated wires) is a subject well-covered in the literature.[1...13]

---

[*]For a beam width of 1°, the Fresnel region extends as far as ~100 m at a wavelength $\lambda = 3$ cm, and as far as ~1000 m at $\lambda = 3$ mm.

In particular the "Special Issue on Radar Reflectivity" of the Proceedings of the IEEE,[4] contains a comprehensive bibliography on this subject. The incident field in these publications is usually assumed to be a plane wave.* If the wire is of finite length and if it is situated in the far zone of the antenna, the incident field along the wire will indeed approach a plane wave, and knowledge of the plane wave scattering properties would permit immediate determination of the radar cross-section of the wire. The received backscatter power is readily obtained from the radar cross-section if the antenna radiation characteristic is known. However, for very long wires such as are treated here, calculation of the radar response requires decomposition of the antenna beam into its directional spectrum of elementary plane waves, solution of the scatter problem for the individual elementary waves, and superposition of the contributions from all these elementary waves to the received backscatter power. We show in this paper that if the wire is situated in the far field region of the antenna the radar response is still determined essentially by only one plane wave, the elementary wave propagating in the direction which intersects the wire axis at right angles. If the wire crosses the Fresnel region, all elementary waves contribute to the radar response. In this report the radar response is derived and evaluated for Gaussian antennas.

2. BACKSCATTER POWER RETURNED TO TRANSMITTING ANTENNA

Consider a horn antenna radiating in the presence of a metallic scatter object (see Fig. 1). We denote the primary field which the antenna would emit if the scatterer were absent by $\vec{E}_p$, $\vec{H}_p$. Diffraction of this primary field at the scatterer produces a secondary field $\vec{E}_s$, $\vec{H}_s$. This secondary field generates a tertiary field at the antenna, which in turn is diffracted at the scatterer, etc. The tertiary field and all subsequent field terms are combined into a rest field $\vec{E}_R$, $\vec{H}_R$. The primary, secondary, and the rest fields satisfy the boundary conditions:

$$ (\vec{E}_p)_{tang} = 0 \quad and \quad (\vec{E}_s + \vec{E}_R)_{tang} = 0 \tag{1a} $$

$$ (\vec{E}_p + \vec{E}_s)_{tang} = 0 \quad and \quad (\vec{E}_R)_{tang} = 0 \tag{1b} $$

---

*Exceptions for instance are papers [12] and [13] in which dipole excitation is assumed.
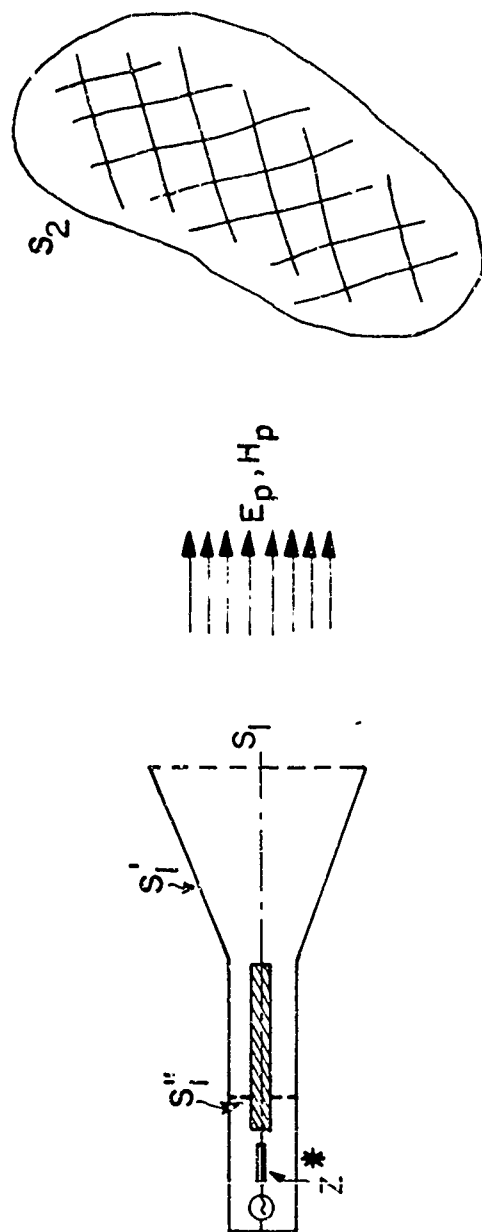
FIG. 1. Horn antenna radiating in presence of scatter object.

The sources of the primary field are located at the antenna; the sources of the secondary field at the scatterer. The rest field has sources at both locations. All three fields satisfy the radiation condition provided the scatter object has finite dimensions. The wire-scatterer treated in this paper is assumed to be of arbitrary but still finite length.

The reciprocity theorem states that any two fields $\vec{E}_1$, $\vec{H}_1$ and $\vec{E}_2$, $\vec{H}_2$ satisfy the relation

$$\oint_S \left\{ \vec{E}_1 \times \vec{H}_2 - \vec{E}_2 \times \vec{H}_1 \right\} d\vec{\sigma} = 0 \tag{2}$$

provided the surface S incloses a space range free of sources. We assign

$$\vec{E}_1, \vec{H}_1 = \vec{E}_P, \vec{H}_P \quad and \quad \vec{E}_2, \vec{H}_2 = \vec{E}_S + \vec{E}_R, \vec{H}_S + \vec{H}_R$$

and apply equation (2) to the space range outside the antenna and the scatter object. The surface S in this case consists of three parts: A sphere of radius $R \to \infty$ which does not contribute to the reciprocity integral since all partial fields satisfy the radiation condition; the surface S_2 of the scatter object; and the aperture S_1 and the metallic wall S_1' of the antenna. Because of boundary conditions (1a), the integral over the surface S_1' is zero. Using boundary conditions (1b), we obtain

$$\int_{S_1} \left\{ \vec{E}_P \times (\vec{H}_S + \vec{H}_R) - (\vec{E}_S + \vec{E}_R) \times \vec{H}_P \right\} d\vec{s}$$

$$= - \oint_{S_2} \left\{ \vec{E}_P \times (\vec{H}_P + \vec{H}_S + \vec{H}_R) \right\} d\vec{s} \tag{3}$$

We further apply the reciprocity theorem to the closed surface formed by the antenna aperture S_1, the inner antenna wall, and a cross-section S_1'' of the

4

coaxial part of the antenna near the feed point. It can be shown that [14]

$$\int_{S_1} \left\{ \vec{E}_P \times (\vec{H}_s + \vec{H}_R) - (\vec{E}_s + \vec{E}_R) \times \vec{H}_P \right\} d\vec{s}$$

$$= V_t I_r + V_r I_t = (Z + Z^*) I_t I_r \tag{4}$$

where V_t and I_t are voltage and current at S_1'' associated with the unperturbated transmitter field, and V_r, I_r are the corresponding quantities for the received backscatter field. Z is the input impedance of the antenna (at S_1'') to which the receiver impedance Z^* is assumed to be matched. By combining equations (3) and (4), we can express the product $I_r I_t$ by an integral over the surface of the scatter object

$$(Z + Z^*) I_t I_r = -\oint_{S_2} \left\{ \vec{E}_P \times (\vec{H}_P + \vec{H}_R + \vec{H}_S) \right\} d\vec{s} \tag{5}$$

where for all practical purposes $\vec{H}_R$ on the right side can be neglected because the rest field, which is generated by diffraction of the secondary field at the antenna, is very weak at the scatterer.

The power radiated by the antenna in the absence of a scatterer is

$$N_t = \frac{1}{2} (Z + Z^*) I_t I_t^* = \frac{1}{2} \int_{S_1} \left\{ \vec{E}_P \times \vec{H}_P^* + \vec{E}_P^* \times \vec{H}_P \right\} d\vec{s} \tag{6}$$

5

and the power received from the backscatter field is

$$N_r = \frac{1}{2} (Z + Z') I_r I_r^*$$

The asterisks indicate conjugate complex values. Hence with equation (5), the ratio of received and transmitted power can be written

$$\eta = \frac{N_r}{N_t} = \frac{1}{4} \frac{Q Q^*}{N_t^2} \tag{7}$$

where Q is the reciprocity integral (5) in which the term $\vec{H}_R$ has been omitted:

$$Q = \oint_{S_2} \{ \vec{E}_P \times (\vec{H}_P + \vec{H}_S) \} d\vec{6} \tag{8}$$

3. PLANE WAVE REPRESENTATION OF INCIDENT FIELD

We formulate the primary field $\vec{E}_p$, $\vec{H}_p$ and derive (in Section 4) the secondary field $\vec{E}_s$, $\vec{H}_s$ for the problem of a Gaussian beam illuminating a straight metallic wire. Figure 2 shows the geometrical arrangement. For convenience, we shall use a cartesian and a cylindrical coordinate system simultaneously. The common z-axis of the two systems is the wire axis. The x-axis, from which the angular coordinate φ is counted, connects the center of the antenna aperture with the wire axis. The radial coordinate is, as usual, defined by $\rho = \sqrt{x^2 + y^2}$. The plane x = -d is a mathematical surface perpendicular to the x-axis just in front of the antenna aperture.

We split the primary antenna field into two parts, one derived from an electric vector potential and the other derived from a magnetic vector potential. These vector potentials can be assumed to comprise only a z-component which we will denote as $\mathfrak{f}_p$ and $\mathfrak{f}_p$, respectively. The electric and magnetic

6
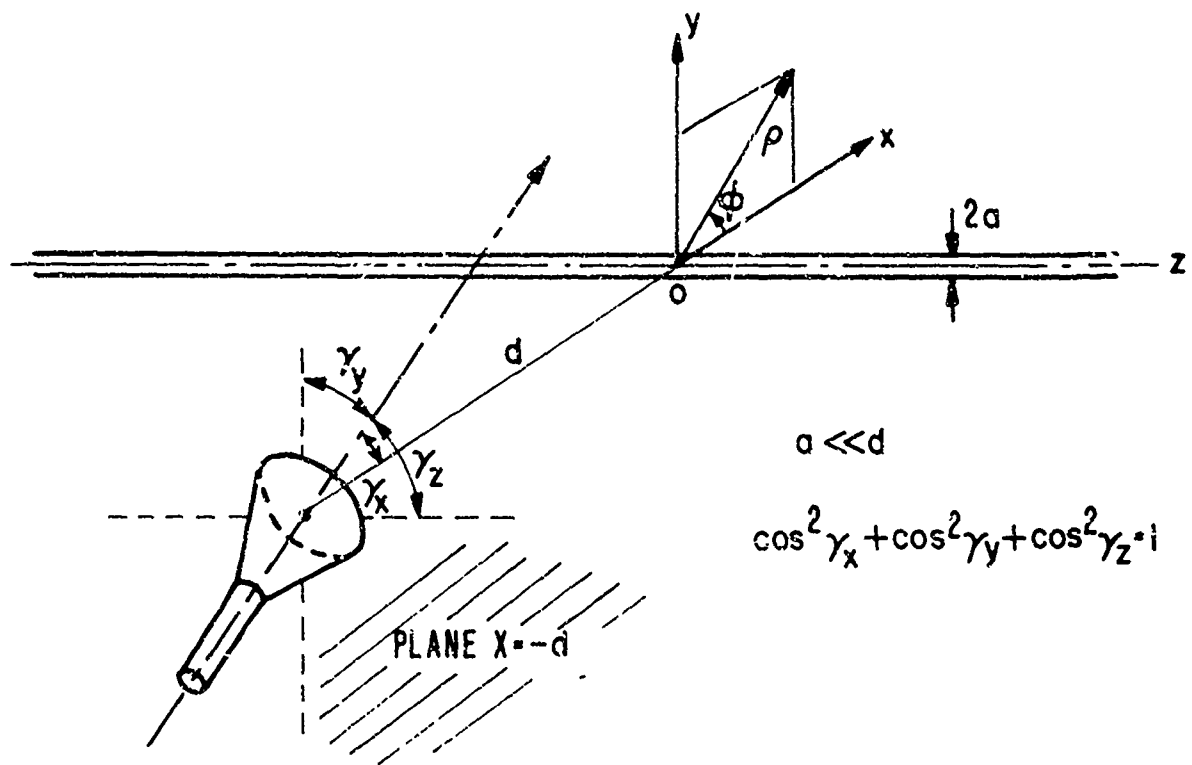
FIG. 2. Coordinate systems used in treating problem of straight metallic wire illuminated by horn antenna.

field strengths are obtained from ϕ_p and ψ_p according to the relations

$$\vec{E}_p = \operatorname{curl}\,\operatorname{curl}\,(\bar{\phi}_p\,\vec{e}_z) - ik\,\operatorname{curl}\,(\psi_p\vec{e}_z)$$

$$\sqrt{\frac{\mu}{\varepsilon}}\,\vec{H}_p = \operatorname{curl}\,\operatorname{curl}\,(\psi_p\vec{e}_z) + ik\,\operatorname{curl}\,(\bar{\phi}_p\,\vec{e}_z)$$

(9)

where $\vec{e}_z$ is the unit vector of the z-direction, and $k = 2\pi/\lambda$ is the wave number. Note that $E_z = 0$ for the partial field derived from the potential ϕ_p, and $E_z = 0$ for the partial field derived from the potential ψ_p. Both vector potentials satisfy the wave equation and in the half-space, $x > -d$ can be written as superpositions of elementary plane waves:

$$\phi_p(x,y,z) = \iint\limits_{h_y,h_z=-\infty}^{+\infty} f(h_y,h_z)\,\exp\left\{-ik\left[h_x(x+d)+h_y\,y+h_z\,z\right]\right\}dh_y\,dh_z$$

(10)

$$\psi_p(x,y,z) = \iint\limits_{h_y,h_z=-\infty}^{+\infty} g(h_y,h_z)\,\exp\left\{-ik\left[h_x(x+d)+h_y\,y+h_z\,z\right]\right\}dh_y\,dh_z$$

$$\text{where}\quad h_x = \sqrt{1-h_y^2-h_z^2}\quad \text{for}\quad h_y^2+h_z^2 \leq 1$$

$$= -i\sqrt{h_y^2+h_z^2-1}\quad \text{for}\quad h_y^2+h_z^2 \geq 1$$

In the range where h_x is real the elementary plane waves are of the propagating type, and in the range where h_x is imaginary they are of the evanescent type in respect to the x-direction. The amplitude spectra $f(h_y, h_z)$ and $g(h_y, h_z)$ according to equations (10) are the Fourier transforms of the

8

distributions of Φ_p and ψ_p in the plane $x = -d$. Applying the inverse transformation we obtain:

$$f(h_y, h_z) = \frac{k^2}{4\pi^2} \iint\limits_{y,z=-\infty}^{+\infty} \bar{E}_p(-d, y, z) \exp\{+ik(h_y y + h_z z)\}\, dy\, dz \tag{11}$$

$$g(h_y, h_z) = \frac{k^2}{4\pi^2} \iint\limits_{y,z=-\infty}^{+\infty} \bar{\psi}_p(-d, y, z) \exp\{+ik(h_y y + h_z z)\}\, dy\, dz$$

As stated before, we shall deal specifically with the case that the primary field radiated by the antenna is a Gaussian beam. The reference plane of the beam (waist of the beam)[15] is assumed to be situated in the aperture plane of the antenna. When the antenna is directed toward the wire so that the beam axis coincides with the x-axis (vertical incidence), the reference plane is the plane $x = -d$ and the field distribution at $x = -d$ is either

$$\bar{E}_z = -\sqrt{\frac{\mu}{\varepsilon}}\, H_y = E_o \exp\left\{-\frac{1}{2}\frac{y^2 + z^2}{\rho_o^2}\right\} \tag{12a}$$

or

$$\bar{E}_y = +\sqrt{\frac{\mu}{\varepsilon}}\, H_z = E_o \exp\left\{-\frac{1}{2}\frac{y^2 + z^2}{\rho_o^2}\right\} \tag{12b}$$

depending on whether the magnetic or the electric field strength is polarized normal to the direction of the wire axis. The mode parameter of the beam is ρ_o. Tilting of the beam axis against the x-axis leads to modification of the field distribution in the plane $x = -d$. The modified field distribution

9

in the former case ($H_z = 0$) is approximately given by:

$$E_x = - E_o V(y,z) \cos\gamma_y \, \mathrm{cotg}\,\gamma_z \qquad \sqrt{\tfrac{\mu}{\varepsilon}}\, H_x = + E_o V(y,z)\, \frac{\cos\gamma_y}{\sin\gamma_z}$$

$$E_y = - E_o V(y,z) \cos\gamma_y \, \mathrm{cotg}\,\gamma_z \qquad \sqrt{\tfrac{\mu}{\varepsilon}}\, H_y = - E_o V(y,z)\, \frac{\cos\gamma_x}{\sin\gamma_z} \qquad (13a)$$

$$E_z = + E_o V(y,z) \qquad\qquad\qquad \sqrt{\tfrac{\mu}{\varepsilon}}\, H_z = 0$$

and the modified distribution in the latter case ($E_z = 0$) by

$$E_x = - E_o V(y,z)\, \frac{\cos\gamma_y}{\sin\gamma_z} \qquad \sqrt{\tfrac{\mu}{\varepsilon}}\, H_x = - E_o V(y,z) \cos\gamma_x \, \mathrm{cotg}\,\gamma_z$$

$$E_y = + E_o V(y,z)\, \frac{\cos\gamma_x}{\sin\gamma_z} \qquad \sqrt{\tfrac{\mu}{\varepsilon}}\, H_y = - E_o V(y,z) \cos\gamma_y \, \mathrm{cotg}\,\gamma_z \qquad (13b)$$

$$E_z = 0 \qquad\qquad\qquad\qquad \sqrt{\tfrac{\mu}{\varepsilon}}\, H_z = + E_o V(y,z) \sin\gamma_z$$

where

$$V(y,z) = \exp\left\{ -\tfrac{1}{2}\, \frac{y^2 \sin^2\gamma_y + z^2 \sin^2\gamma_z}{\rho_o^2} - ik\,(y \cos\gamma_y + z \cos\gamma_z) \right\} \qquad (13c)$$

10

The angles which the beam axis forms with the x,y,z-directions are γ_x, γ_y, γ_z respectively (see Fig. 2); obviously

$$\cos^2\gamma_x + \cos^2\gamma_y + \cos^2\gamma_z = 1$$

The phase term in equation (13c) describes the tilt of the phase fronts of the beam against the plane x = -d, and the factors $\sin^2\gamma_y$ and $\sin^2\gamma_z$ in the real part of the exponent describe the broadening of the amplitude distribution of the beam in the plane x = -d with increasing tilt angle. It is readily seen that for $\gamma_x \rightarrow 0$ field distributions (13a) and (13b) approach distributions (12a) and (12b) respectively. For all tilt angles these field distributions satisfy the relations:

$$\vec{E} = \sqrt{\frac{\mu}{\varepsilon}}\, \vec{n} \times \vec{H} \qquad and$$

$$|\vec{E}| = \sqrt{\vec{E}\cdot\vec{E}^*} = E_o|V| = E_o \exp\left\{-\frac{1}{2}\frac{y^2\sin^2\gamma_y + z^2\sin^2\gamma_z}{\rho_o^2}\right\}$$

where $\vec{n}$ is the unit vector in the direction of the beam axis. $\vec{E}$, $\vec{H}$, and $\vec{n}$ in other words are mutually orthogonal for all γ_y, γ_z, and $|\vec{E}|$ as well as $|\vec{H}|$ does not vary with γ_y, γ_z except for a change in the coordinate scale.

Equations (13) are approximations only for the actual distribution of a tilted Gaussian beam in the plane x = -d. However, the smaller γ_x is, the better the approximation. In the following, we shall assume that the antenna radiates a rather narrow beam with a beam width in the order of 1°. The back-scatter power received by the antenna then decreases rapidly as the beam axis is tilted against the direction $\gamma_x = 0$ ($\gamma_y, \gamma_z = 90^o$), and we can restrict our considerations to a small angular range about this direction, where equations (13) describe the actual field distribution with sufficient accuracy.

The radiation characteristic $R(\theta)$ of a Gaussian beam (12) is proportional to

$$R(\theta) \sim e^{-(k\rho_0)^2 \sin^2\theta}$$

where θ is the angular deviation of the direction of observation from the beam axis. A beam width of 1° for instance would require $k\rho_0 \approx 100$.

The fields determined by equations (13a) and (13b) can be derived from electric and magnetic vector potentials Φ_p and Ψ_p, respectively whose distributions in the plane $x = -d$ are given in good approximation by:

$$\Phi_p(-d, y, z), \quad \Psi_p(-d, y, z) = \frac{E_0}{k^2 \sin\gamma_z} V(y, z) \tag{14}$$

The corresponding amplitude functions are obtained with equations (11):

$$f(h_y, h_z), g(h_y, h_z) = \frac{(k\rho_0)^2}{2\pi} \frac{1}{\sin\gamma_y \sin^2\gamma_z} \exp\left\{-\frac{1}{2}(k\rho_0)^2\left[\left(\frac{h_y - \cos\gamma_y}{\sin\gamma_y}\right)^2 + \left(\frac{h_z - \cos\gamma_z}{\sin\gamma_z}\right)^2\right]\right\} \tag{15}$$

With $k\rho_0$ in the order of 100, the amplitude functions f and g have appreciable values in only a very small h_y, h_z-range about the point $h_y = \cos\gamma_y$, $h_z = \cos\gamma_z$. Therefore the integration in equations (10) for Φ_p and Ψ_p, and in the expressions obtained with equations (9) for the field strength components can be essentially restricted to a neighborhood of this point. Calculating the field distribution in the plane $x = -d$ in this manner indeed reproduces the field strength components (13a) and (13b). Hence the vector potentials Φ_p and Ψ_p obtained by inserting the amplitude functions (15) into equations (10) describe the desired Gaussian beams of variable axis directions, at least in the interesting range of small γ_x. The electric vector potential characterizes a beam whose magnetic field strength is polarized normal to the wire axis direction ($H_z = 0$), and the magnetic vector potential characterizes a beam whose electric field strength is polarized normal to this direction ($E_z = 0$).

12

The power N, transmitted in a field (10) can be expressed in terms of the absolute square amplitude spectra of the propagating elementary waves.[16] Fields derived from the potentials ϕ and ψ are mutually orthogonal with regard to the transmitted power. Hence

$$N_z = V_\phi + N_\psi \tag{16}$$

where

$$N_\phi = 4\pi^2 \sqrt{\frac{\varepsilon}{\mu}} k^2 \iint_{h_y^2 + h_z^2 \leq 1} f(h_y, h_z) f^*(h_y, h_z) h_x (1 - h_z^2) \, dh_y \, dh_z \tag{16a}$$

$$N_\psi = 4\pi^2 \sqrt{\frac{\varepsilon}{\mu}} k^2 \iint_{h_y^2 + h_z^2 \leq 1} g(h_y, h_z) g^*(h_y, h_z) h_x (1 - h_z^2) \, dh_y \, dh_z \tag{16b}$$

For the example of a Gaussian beam, amplitude spectra (15) must be inserted into equations (16). Since $k\rho_0$ is a large number, the integration can be performed approximately with the result

$$N_\phi, N_\psi = \pi \sqrt{\frac{\varepsilon}{\mu}} k^4 \rho_0^2 \frac{\cos \gamma_x}{\sin \gamma_y \sin \gamma_z}$$

The relative error is in the order of $(k\rho_0)^{-2}$. Considering only directions of the beam axis which do not deviate substantially from the direction

13

of vertical incidence ($\gamma_x \approx 0$), we may further approximate

$$\cos \gamma_x = \left\{ \sin^2 \gamma_y \sin^2 \gamma_z - \cos \gamma_y \cos \gamma_z \right\}^{\frac{1}{2}} \approx \sin \gamma_y \sin \gamma_z$$

and hence

$$N_{\bar{z}}, N_y = \tau \sqrt{\frac{\varepsilon}{\mu}} \, k^4 \rho_0^{\,2} \tag{17}$$

For an angular deviation from vertical incidence of, for instance, $15°$ the relative error is still below $1/400$.

4. CYLINDER WAVE REPRESENTATION OF SCATTER FIELD

Equation (15) shows that the amplitude spectra f and g of a Gaussian beam of narrow beam width are practically zero in the range of evanescent elementary waves. Since furthermore these evanescent waves decrease exponentially with increasing distance from the reference plane $x = -d$, their contributions to the incident field at the wire can be neglected. In the range of propagating elementary waves, we substitute in equations (10)

$$h_x = \cos \alpha \, \sin \beta, \quad h_y = \sin \alpha \, \sin \beta, \quad h_z = \cos \beta$$

The geometrical meaning of α and β is illustrated in Fig. 3. β is the angle which the direction of propagation of any elementary wave includes with the z-axis and α is the projected angle against the x-direction. Hence
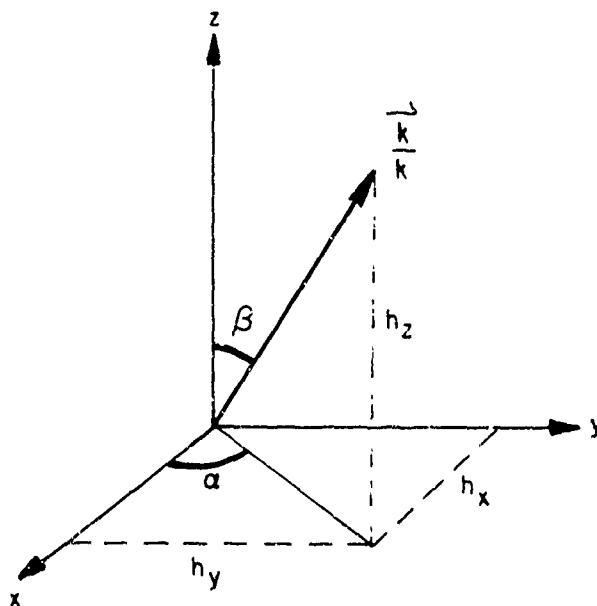
14

FIG. 3. Geometrical relation between angles α, β and directional cosines h_x, h_y, h_z characterizing direction of propagation of elementary plane wave.

expressions (10) for Φ_p and Ψ_p become:

$$\overline{\Phi}_p(\rho,\varphi,z) = \int\limits_{\alpha=-\frac{\pi}{2},\beta=0}^{+\frac{\pi}{2}}\int\limits^{\pi} f(\sin\alpha\sin\beta,\cos\beta)\exp\left\{-ik\left[d\cos\alpha\sin\beta + \rho\cos(\varphi-\alpha)\sin\beta + z\cos\beta\right]\right\} \cdot$$

$$\cdot \cos\alpha\sin^2\beta\, d\alpha\, d\beta \tag{18}$$

$$\overline{\Psi}_p(\rho,\varphi,z) = \int\limits_{\alpha=-\frac{\pi}{2},\beta=0}^{+\frac{\pi}{2}}\int\limits^{\pi} q(\sin\alpha\sin\beta,\cos\beta)\exp\left\{-ik\left[d\cos\alpha\sin\beta + \rho\cos(\varphi-\alpha)\sin\beta + z\cos\beta\right]\right\} \times$$

$$\times \cos\alpha\sin^2\beta\, d\alpha\, d\beta$$

where x and y have been replaced by the cylindrical coordinates ρ and φ (see Figure 2).

The elementary plane wave

$$\overline{\Phi}_i, \Psi_i = \exp\left\{-ik\left[\rho\cos(\varphi-\alpha)\sin\beta + z\cos\beta\right]\right\} \tag{19}$$

when incident upon a straight wire (whose axis coincides with the z-axis) produces a scatter field that can be written as a superposition of elementary cylindrical waves:

$$\overline{\Phi}_r, \Psi_r = \sum_{m=-\infty}^{+\infty} c_m^{(\Phi,\Psi)} H_m^{(2)}(k\rho\sin\beta)\, e^{im(\varphi-\alpha)}\, e^{-ikz\cos\beta} \tag{20}$$

The expansion coefficients $c_m^{(\Phi)}$ and $c_m^{(\Psi)}$ are obtained from the boundary

16

conditions which, for a metallic wire of radius a, are

$$\left(\bar{\Phi}_c + \bar{\Phi}_r \right)_{\rho=a} = C \qquad and \qquad \left(\frac{\partial \bar{\Phi}_c}{\partial S} + \frac{\partial \bar{\Phi}_r}{\partial \rho} \right)_{\rho=a} = C \qquad (21)$$

respectively. Using the cylinder function representation of a plane wave[17]

$$e^{-ik\rho\cos(\varphi-\alpha)\sin\beta} = \sum_{m=-\infty}^{+\infty} J_m(k\rho\sin\beta)\, e^{im(\varphi - x - \frac{\pi}{2})}$$

we immediately find that:

$$c_m^{(\bar{\Phi})} = -e^{-im\frac{\pi}{2}}\, \frac{\bar{J}_m(ka\sin\beta)}{H_m^{(2)}(ka\sin\beta)}$$

$$and \qquad c_m^{(\Psi)} = -e^{-im\frac{\pi}{2}}\, \frac{J_m'(ka\sin\beta)}{H_m^{(2)'}(ka\sin\beta)} \qquad (22)$$

where J_m', $H_m^{(2)'}$ are the derivatives of J_m, $H_m^{(2)}$ with regard to the argument. The total scatter field produced by diffraction of the incident field (18) at the wire is obviously obtained by superposition of the contributions (20)

17

from all incident elementary waves (19)

$$\bar{\Phi}_S(\rho,\varphi,z) = -\int\limits_{\alpha=-\frac{\pi}{2},\,\beta=0}^{\frac{\pi}{2}}\int\limits_{}^{\pi} f(\sin\alpha\sin\beta,\cos\beta)\exp\{-ik[d\cos\alpha\sin\beta + z\cos\beta]\}\cdot$$

$$\cdot\sum_{m=-\infty}^{+\infty} \frac{J_m(ka\sin\beta)}{H_m^{(2)}(ka\sin\beta)}\,\dot{H}_m^{(2)}(k\rho\sin\beta)\,e^{im(\varphi-\alpha-\frac{\pi}{2})}\cos\alpha\sin^2\beta\,d\alpha\,d\beta$$

$$(23)$$

$$\tilde{\Psi}_S(\rho,\varphi,\bar{z}) = -\int\limits_{\alpha=-\frac{\pi}{2},\,\beta=0}^{+\frac{\pi}{2}}\int\limits_{}^{\pi} g(\sin\alpha\sin\beta,\cos\beta)\exp\{-ik[d\cos\alpha\sin\beta + z\cos\beta]\}\cdot$$

$$\times\sum_{m=-\infty}^{+\infty} \frac{J_m^{\prime}(ka\sin\beta)}{H_m^{(2)\prime}(ka\sin\beta)}\,H_m^{(2)}(k\rho\sin\beta)\,e^{im(\varphi-\alpha-\frac{\pi}{2})}\cos\alpha\sin^2\beta\,d\alpha\,d\beta$$

In the case of Gaussian illumination, the amplitude functions f and g are given by equation (15).

5. DISCUSSION OF THE SCATTER FIELD

First we will discuss the case of a wire situated in the far field region of the antenna. The exponential function exp{-ik (dcosαsinβ + zcosβ)} in the integrand of equations (23) then varies much more rapidly with α and β than do the amplitude functions f(sinαsinβ, cosβ) and g(sinαsinβ, cosβ). As a consequence, the integration can be carried out asymptotically using the method

18

of stationary phase:

$$\Phi_S(\rho,\varphi,z) = 2\sqrt{2r'}\,\frac{e^{-i(kr+\frac{\pi}{4})}}{\sqrt{k^3 d\varphi r}}\,f(0,\cos\theta)\sin\theta\sum_{m=-\infty}^{+\infty}\frac{J_m(ka\sin\theta)}{H_m^{(2)}(ka\sin\theta)}\,e^{im\varphi}$$

(24)

$$\Psi_S(\rho,\varphi,z) = 2\sqrt{2r'}\,\frac{e^{-i(kr+\frac{\pi}{4})}}{\sqrt{k^3 d\varphi r}}\,g(0,\cos\theta)\sin\theta\sum_{m=-\infty}^{+\infty}\frac{J_m'(ka\sin\theta)}{H_m^{(2)'}(ka\sin\theta)}\,e^{im\varphi}$$

$$\text{where}\quad r = \{(\rho+d)^2+z^2\}^{\frac{1}{2}}\,,\quad tg\,\theta = \frac{\rho+d}{z}$$

Before applying the method of stationary phase, the Hankel functions $H_m^{(2)}$ (kρ=a) in the integrands of equations (23) were replaced by their asymptotic representations. When the immediate vicinity of the wire[*] is disregarded, this is permissible for all m for which the terms under the summation sign are of appreciable magnitude.

The geometrical meaning of the new variables r and θ is illustrated in Fig. 4. The shortest line which joins the point of observation ρ, φ, z with the center of the antenna aperture and simultaneously crosses the wire axis consists of two straight line sections, r_1 and r_2. Both form the angle θ with the z-direction; their combined length is the variable r. Note that r and θ do not depend on the azimuth angle φ.

Points of observation characterized by identical values of θ obviously form conical surfaces (with vertex angle θ) about the wire axis, the vertex itself being located at z = z_0 = d·cotgθ. According to equations (24), the distribution of the scatter fields Φ_S and Ψ_S along a given surface θ = const is determined by the values of the amplitude functions f and g of the incident

[*] i.e., assuming ρ > 5a for thick wires and ρ > 5 λ for thin wires, where a is the wire radius and λ the wavelength.

19

$P(\rho, \phi, z)$

$z_0 = d\cot\theta$

$r = r_1 + r_2 = \{(d+\rho)^2 + z^2\}^{\frac{1}{2}}$

$tg\,\theta = \dfrac{d+\rho}{z}$

FIG. 4.   Coordinates r and θ used in describing scatter field of straight wire.

20

beam for one direction α, β only, the direction

$$\alpha = 0 \quad , \quad \beta = \theta \tag{25}$$

In other words, only one of the elementary plane waves of the incident beam contributes significantly to the field scattered by the wire along a cone θ = const. According to equation (25), the direction of propagation of this wave points from the antenna center towards the wire intersecting the wire axis at the angle θ (line r_1 in Fig. 4).

By inserting amplitude spectra (15) into equations (24), we obtain for the example of a Gaussian beam:

$$\bar{\Phi}_s(\varsigma,\varphi,z) = \bar{\Phi}_1(\varphi, \theta(\varsigma,z)) \bar{\Phi}_2(\varrho,z) \quad , \quad \tilde{\Psi}_s(\varrho,\varphi,z) = \tilde{\Psi}_1(\varphi, \theta(\varsigma,z)) \tilde{\Psi}_2(\varrho,z)$$

where

$$\bar{\Phi}_1(\varphi,\theta) = \sum_{m=-\infty}^{+\infty} \frac{J_m(ka\sin\theta)}{H_m^{(2)}(ka\sin\theta)} e^{im\varphi}$$

$$\tilde{\Psi}_1(\varphi,\theta) = \sum_{m=-\infty}^{+\infty} \frac{J_m'(ka\sin\theta)}{H_m^{(2)\prime}(ka\sin\theta)} e^{im\varphi} \tag{26}$$

and

$$\bar{\Phi}_2(\varrho,z) = \tilde{\Psi}_2(\varsigma,z) = \sqrt{\frac{2}{\pi}} \frac{(k\varsigma_0)^2 \sin\theta}{\sqrt{k^3 d\varsigma r} \; \sin\gamma_1 \sin^2\gamma_z} \times$$

$$\times \exp\left\{-i\left(kr + \frac{\pi}{4}\right) - \frac{1}{2}(k\varsigma_0)^2\left[\cot g^2\gamma_1 + \left(\frac{\cos\theta - \cos\beta}{\sin\gamma_z}\right)^2\right]\right\}$$

21

$$\text{with} \quad r = \left\{ (\rho + d)^2 + z^2 \right\}^{\frac{1}{2}}, \quad tg\, \epsilon = \frac{\rho + d'}{z}$$

Since $k\rho_0$ is assumed to be large, the exponential function in the expressions for ϕ_2, ψ_2 decreases rapidly as θ deviates from γ_z. In other words, the scatter field is concentrated near the conical surface $\theta = \gamma_z = \text{const}$. In the neighborhood of this surface we may substitute γ_z for θ in the expressions for ϕ_1 and ψ_1:

$$\bar{\Phi}_1(\varphi, \theta) \approx \bar{\Phi}_1(\varphi, \gamma_z) = \sum_{m=-\infty}^{+\infty} \frac{J_m(ka\sin\gamma_z)}{H_m^{(2)}(ka\sin\gamma_z)} e^{im\varphi}$$

$$\Psi_1(\varphi, \theta) \approx \Psi_1(\varphi, \gamma_z) = \sum_{m=-\infty}^{+\infty} \frac{J_m'(ka\sin\gamma_z)}{H_m^{(2)'}(ka\sin\gamma_z)} e^{im\varphi}$$

(27)

With this approximation, ϕ_1 and ψ_1 no longer depend on ρ and z, and equations (26) represent the scatter fields, ϕ_s and ψ_s, as products of a function depending only on the azimuth angle φ and a function depending only on the radial and axial coordinates ρ and z. Hence, in any plane through the wire axis ($\varphi = \text{const}$), the scatter field ϕ_s (or ψ_s) has essentially the same distribution except for an amplitude factor which varies from plane to plane according to the function ϕ_1 (or ψ_1).

In the case the wire crosses the Fresnel region of the antenna, the exponential function $\exp\{-ik(d\cos\alpha\sin\beta + z\cos\beta)\}$ in the integrand of equations (23) varies with α, β at a rate comparable to the rate of change of the amplitude functions f and g, and an asymptotic evaluation of the integrals is no longer permissible. Inspection of the location of the stationary points of exponential function and amplitude spectra shows that for a Gaussian beam, however, the expressions ϕ_s and ψ_s can be simplified so that the scatter fields can

22

still be written in the product form (26) where Φ_1 and Ψ_1, as before, are approximately given by equations (27) and

$$\bar{\Phi}_2(\bar{\rho},\bar{z}),\ \bar{\Psi}_2(\bar{\rho},\bar{z}) \approx -\frac{(k\rho_0)^2 e^{i\frac{z}{r}}}{\sqrt{2\pi^3 k\rho}\ \sin\gamma_y \sin\frac{\gamma_z}{2}} \times$$

$$\times \int_{\alpha=-\frac{\pi}{2}}^{+\frac{\pi}{2}}\int_{\beta=0}^{\bar{z}} \exp\Big\{-ik(d\cos\alpha\sin\beta + \rho\sin\beta + z\cos\beta)$$

$$-\frac{1}{2}(k\rho_0)^2\Big[\Big(\frac{\sin\alpha\sin\beta-\cos\gamma_y}{\sin\gamma_y}\Big)^2 + \Big(\frac{\cos\beta-\cos\gamma_z}{\sin\gamma_z}\Big)^2\Big]\Big\}$$

$$\times \cos\alpha\sin^{3/2}\beta\ d\alpha\ d\beta$$

(28)

The Hankel functions $H_m^{(2)}$ ($k\rho\sin\beta$) in the integrand were again approximated by their asymptotic representations and the beam axis angles γ_y and γ_z were assumed to be in the vicinity of 90° (nearly vertical incidence). The result obtained for a wire in the antenna far zone - that the scatter field in any plane through the wire axis has approximately the same distribution - therefore holds for a wire in the Fresnel region of the antenna as well. However, the field distribution along a surface θ = const is no longer determined by only one elementary plane wave of the incident beam, but as one would expect, by the entire elementary wave spectrum, or at least a substantial portion of it.

6. RECIPROCITY INTEGRAL FOR STRAIGHT METALLIC WIRES

We formulate the reciprocity integral Q, equation (8), for a straight metallic wire. Integration in equation (8) is performed over the wire surface ρ = a (see Fig. 2); the surface element is accordingly given by $d\sigma = a\,d\varphi\,dz$. Using equations (9), the field strengths $\bar{E}_\rho$, $\bar{H}_\rho$, and $\bar{H}_s$ occurring in the integrand of Q can be expressed in terms of the vector potentials Φ_p, Ψ_p and Φ_s, Ψ_s respectively. For a field derived from the electric vector potential we obtain

$$Q_z = ika\sqrt{\frac{\varepsilon}{\mu}}\int_{z=-\infty}^{+\infty}\int_{\varphi=0}^{2\pi}\Big\{(k^2\bar{\Phi}_\rho + \frac{\partial^2\bar{\Phi}_\rho}{\partial z^2})\frac{\partial}{\partial\rho}(\bar{\Phi}_\rho + \bar{\Phi}_s)\Big\}_{\rho=a} d\varphi\,dz \quad (39a)$$

23

and for a field derived from the magnetic vector potential, we obtain:

$$Q_{\psi} = \iota ka \sqrt{\frac{\epsilon}{\mu}} \int_{z=-\infty}^{+\infty} \int_{\varphi=c}^{2\pi} \left\{ \frac{\partial \psi_p}{\partial \rho} \left[k^2 (\psi_p + \psi_s) + \frac{\partial^2}{\partial z^2} (\psi_p + \psi_s) \right] \right\}_{\rho=a} d\varphi\, dz \quad (29b)$$

If the field is characterized by both vector potentials, the reciprocity integral is the sum of expressions (29a) and (29b) since there is no interaction in regard to Q between fields derived from the potentials Φ and ψ:

$$Q = Q_{\Phi} + Q_{\psi} \quad (29c)$$

We insert Φ_p, ψ_p and Φ_s, ψ_s according to equations (18) and (23) into equations (29). Using the orthogonality properties of the functions $e^{im\varphi}$, the φ-integration can be performed. The z-integration moreover leads to a δ-function:

$$\frac{k}{2\pi} \int_{-\infty}^{+\infty} e^{ikz(\cos\beta + \cos\beta')} dz = \delta(\cos\beta + \cos\beta')$$

so that

$$\int_{c}^{\tau} F(\beta') \, \delta(\cos\beta + \cos\beta') \sin\beta'\, d\beta' = F(\tau - \beta) \qquad \text{for } 0 \leq \beta \leq \tau \quad (30)$$

where $F(\beta)$ is any given function of β. Hence we obtain for the reciprocity

$$Q_E = \left.j - \sqrt{\frac{\varepsilon}{\mu}}\, k^2 \right. \underset{\alpha,\alpha'=-\frac{\pi}{2}}{\overset{+\frac{\pi}{2}}{\iint}} \overset{\pi}{\underset{\beta=0}{\int}} f(\sin\alpha\sin\beta,\cos\beta)\, f(\sin\alpha'\sin\beta,-\cos\beta)\, e^{-jkd(\cos\alpha+\cos\alpha')\sin\beta}$$

$$\times \sum_{m=-\infty}^{+\infty} (-1)^m \frac{J_m(ka\sin\beta)}{H_m^{(2)}(ka\sin\beta)}\, e^{-jm(\alpha-\alpha')} \cos\alpha\cos\alpha'\sin^5\beta\; d\alpha\,d\alpha'\,d\beta \tag{30a}$$

$$Q_{\varphi} = j - \sqrt{\frac{\varepsilon}{\mu}}\, k^2 \underset{\alpha,\alpha'=-\frac{\pi}{2}}{\overset{+\frac{\pi}{2}}{\iint}} \overset{\pi}{\underset{\beta=0}{\int}} g(\sin\alpha\sin\beta,\cos\beta)\, g(\sin\alpha'\sin\beta,-\cos\beta)\, e^{-jkd(\cos\alpha+\cos\alpha')\sin\beta}$$

$$\times \sum_{m=-\infty}^{+\infty} (-1)^m \frac{J_m'(ka\sin\beta)}{H_m^{(2)\prime}(ka\sin\beta)}\, e^{-jm(\alpha-\alpha')} \cos\alpha\cos\alpha'\sin^5\beta\; d\alpha\,d\alpha'\,d\beta \tag{30b}$$

With a later application in mind, we note that expressions (30) for the reciprocity integral Q still hold in general, i.e., for any incident field. In deriving these equations only one approximation has been made; the contribution of the evanescent elementary waves to the incident field at the wire has been neglected. If the distance between antenna and wire is sufficiently large, this omission is obviously justified. For the example of a Gaussian incident beam we obtain by inserting the corresponding amplitude functions (15)

into equations (30)

$$
\left.\begin{array}{c} Q_{\ddot{\phi}} \\[2em] Q_{\gamma} \end{array}\right\} = \frac{2}{\pi} \sqrt{\frac{\varepsilon}{\mu}}\; k^6 \rho_0^4 \; \frac{\exp\left\{-(k\rho_0)^2(\cot g^2 \gamma_j + \cot g^2 \gamma_z)\right\}}{\sin^8 \gamma_j \, \sin^4 \gamma_z} \quad \times
$$

<div align="right">(31a)</div>

<div align="right">(31b)</div>

$$
\times \int\limits_{\alpha,\alpha' = -\frac{\pi}{2}}^{+\frac{\pi}{2}} \int\limits_{\beta = 0}^{\pi} exp\left\{-ik(\cos\alpha + \cos\alpha')\sin\beta - (k\rho_0)^2 \frac{\cos^2\beta}{\sin^2\gamma_z} \right.
$$

$$
\left. - \tfrac{1}{2}(k\rho_0)^2\left[\frac{(\sin\alpha + \sin\alpha')\sin^2\beta}{\sin^2\gamma_j} - 2\frac{(\sin\alpha + \sin\alpha')\sin^2\beta \cos\gamma_j}{\sin^2\gamma_j}\right]\right\}
$$

$$
\times \left\{\begin{array}{c} \displaystyle\sum_{m=-\infty}^{+\infty} (-1)^{m+1}\, \frac{\overline{J_m}(ka\sin\beta)}{H_m^{(2)}(ka\sin\beta)}\, e^{-im(\alpha-\alpha')} \\[2em] \displaystyle\sum_{m=-\infty}^{+\infty} (-1)^{m}\, \frac{J_m'(ka\sin\beta)}{H_m^{(2)\prime}(ka\sin\beta)}\, e^{-im(\alpha-\alpha')} \end{array}\right\} \sin^5\beta \, \cos\alpha \, \cos\alpha' \, d\alpha\, d\alpha'\, d\beta
$$

7. EVALUATION OF RECIPROCITY INTEGRALS Q_ϕ and Q_γ

With the assumptions that the beam width of the incident beam is in the order of $1°$ ($k\rho_0$ in the order of 100) and the beam axis does not deviate substantially (by not more than about $15°$) from the direction of vertical incidence, the reciprocity integrals (31) can be evaluated approximately so that closed form expressions for Q_ϕ and Q_γ are obtained. The method of integration is explained in Appendix A; the result is:

$$
Q_{\phi,\gamma} = 4 \sqrt{\frac{\varepsilon}{\mu}}\; k^3 \rho_0^2 \left(\frac{\iota\varepsilon}{\iota r \iota \varepsilon}\right)^{3/2} \overline{F}_{\phi,\gamma}(ka,\tau) \;\times
$$

<div align="right">(32a)</div>

$$
\times \frac{exp\left\{-2ikd\sqrt{1-u_c^2} - (k\rho_0)^2\left[\left(\frac{u_c - \cos\gamma_j}{\sin\gamma_j}\right)^2 + \cot g^2\gamma_z\right]\right\}}{\sin^2\gamma_j \, \sin^4\gamma_z \, \Gamma(\gamma_j,\gamma_z)}
$$

<div align="center">26</div>

with $\tau = k\rho_0^2/d$ and

$$P(\gamma_j, \gamma_\ell) = 1 + \frac{1}{2} \frac{c\tau}{1+c\tau} \cot^2\gamma_\ell + 2(1 + \frac{3}{4}\frac{c\tau}{(1+c\tau)}) \cot^2\gamma_j) \qquad (32b)$$

$$\approx 1 \qquad \text{for} \quad \gamma_j, \gamma_\ell \approx \frac{\pi}{2} \qquad$$

The parameter u_0 is determined by the equation

$$u_c (1 + \frac{\sin^2\gamma_j}{c\tau\sqrt{1-u_c^2}}) = \cos\gamma_j \qquad (32c)$$

which in Appendix A is solved by a series expansion. Using this expansion, the exponent in equation (32) can be developed into a series of ascending powers of $\cot^2\gamma_Y$. Neglecting 6th and higher order terms, we thus obtain

$$Q_{\Phi,\Psi} = 4\sqrt{\pi}\sqrt{\frac{\varepsilon}{\mu}} k^3\rho_0 (\frac{c\tau}{1+c\tau})^{3/2} \bar{F}_{\Phi,\Psi}(ka,\tau) \frac{1}{\sin^2\gamma_j \sin^4\gamma_\ell P(\gamma_j,\gamma_\ell)} , \qquad (33)$$

$$\cdot \exp\{-i2kd[1 - \frac{1}{2}\frac{\tau^2}{1+\tau^2}\cot^2\gamma_j - \frac{1}{8}\frac{\tau^2}{(1+\tau^2)^4}(4+5\tau^2-k\tau^4-3\tau^6)\cot^4\gamma_j ...]\} \cdot$$

$$\cdot \exp\{-(k\rho_c)^2[\cot^2\gamma_\ell + \frac{1}{1+\tau^2}\cot^2\gamma_j - \frac{\tau^2}{(1+\tau^2)^4}(2+5\tau^2+\tau^4)\cot^4\gamma_j ...]\}$$

The function $F_{\Phi,\Psi}(ka,\tau)$ which determines the dependence of the reciprocity integrals on the wire radius is given by

$$\bar{F}_\Phi(ka,\tau) = \sum_{m=-\infty}^{\infty} (-1)^{m+1} \frac{J_m(ka)}{H_m^{(2)}(ka)} \exp\{- \frac{c\tau}{1+c\tau}(\frac{m}{k\rho_c})^2\} \qquad (34a)$$

27

for a field derived from the electric vector potential ϕ and by

$$\overline{F}_{\psi}(ka,\tau) = \sum_{m=-\infty}^{+\infty} (-1)^m \frac{J_m'(ka)}{H_m^{(2)'}(ka)} \exp\left\{-\frac{i\tau}{1+\tau^2}\left(\frac{m}{k\rho_0}\right)^2\right\} \tag{34b}$$

for a field derived from the magnetic vector potential ψ.

Equations (32) to (34) hold for wires sufficiently thin to satisfy the condition

$$\frac{\tau}{\sqrt{1+\tau^2}}\left(\frac{a}{\rho_0}\right)^2 < 1 \tag{35}$$

This condition, however, does not impose a severe restriction as it admits wire diameters 2a of several wavelengths. If, for instance, $k\rho_0 = 100$ and $\tau = 1$, wire diameters up to 35 λ are permissible. The functions F_ϕ and F_ψ depend weakly on d and ρ_0. This dependence practically disappears as the wire radius a is decreased. If

$$\frac{\tau}{\sqrt{1+\tau^2}}\left(\frac{a}{\rho_0}\right)^2 \ll 1 \tag{36}$$

the exponential factors on the right-hand side of equations (34) can be replaced by unity in all summation terms with $|m| < 2ka$, this means, in all terms of appreciable magnitude. Hence

$$\overline{F}_{\phi}(ka,\tau) \approx \overline{F}_{\phi}(ka,0) = \sum_{m=-\infty}^{+\infty} (-1)^{m+1} \frac{J_m(ka)}{H_m^{(2)}(ka)} \tag{37a}$$

$$\overline{F}_{\psi}(ka,\tau) \approx \overline{F}_{\psi}(ka,0) = \sum_{m=-\infty}^{+\infty} (-1)^m \frac{J_m'(ka)}{H_m^{(2)'}(ka)} \tag{37b}$$

For the above example where $k\rho_0 = 100$ and $\tau = 1$, condition (36) requires that $2a < 10 \lambda$.

If the wire crosses the Fresnel region of the antenna, $\tau = k\rho_0^2/d$ is in the order of or greater than unity. If the wire is situated in the far field region of the antenna, τ is small compared to unity. Hence, according to equation (32c), $u_0 \to 0$ and

$$Q_{\mathcal{E},\varphi} = -4\sqrt{\pi}\,\sqrt{\frac{\varepsilon'}{\mu}}\,k^2 \frac{(k\rho_0)^4}{(kd)^{3/2}}\,\overline{F}_{\mathcal{E},\varphi}(ka,0)\;\frac{\exp\left\{-i(2kd+\frac{\pi}{4})-\sin\gamma_y^2(\cot g^2\gamma_y+\cot g^2\gamma_z)\right\}}{\sin^2\gamma_y\,\sin^4\gamma_z} \quad (38)$$

$F_\phi(ka,0)$ and $F_\psi(ka,0)$ are given by equations (37) which in this case ($\tau \ll 1$) describe the dependence of the reciprocity integrals on wire radius not only for sufficiently thin wires but according to condition (36) for all $(ka)^2 \ll kd$.

The restriction stated at the beginning of this section, that the direction of the beam axis does not substantially deviate from the direction normal to the wire axis has to be imposed only in evaluating the reciprocity integrals for a wire crossing the Fresnel region of the antenna. Even in this case it is not an essential limitation as Q_ϕ and Q_ψ decrease rapidly with increasing deviations of γ_y and γ_z from $90°$. If for example the beam width is $1°$ and $\tau = 1$, and the beam axis deviates from the direction of vertical incidence by not more than $\Delta\gamma_y = 90°-\gamma_y = \pm 3°$ (while $\Delta\gamma_z = 90°-\gamma_z = 0$), the reciprocity integrals Q_ϕ and Q_ψ are already more than 50 dB below their maximum values; if $\Delta\gamma_z = \pm 3°$ (while $\Delta\gamma_y = 0$), they are more than 100 dB below these values. The received backscatter power, which is proportional to QQ^*, decreases correspondingly by more than 100 dB and 200 dB if the beam axis is turned by $\Delta\gamma_y$ or $\Delta\gamma_z = \pm 3°$ against the direction of vertical incidence.

In the case that the wire is situated in the far field region of the antenna, the reciprocity integrals can also be evaluated by a different and more direct method than the one used in Appendix A; an asymptotic evaluation can be performed using the method of stationary phase. This method can be applied to Q_ϕ and Q_ψ in the general form of equations (30) where a particular characteristic of the antenna beam has not yet been specified. The calculations are performed in Appendix B with the result:

$$Q_\phi = -16\,\pi^{5/2}\,\sqrt{\frac{\varepsilon}{\mu}}\,k^2\,\overline{F}_\phi(ka,0)\,\frac{e^{-i(2kd+\frac{\pi}{4})}}{(kd)^{3/2}}\,f^2(0,0) \quad (39a)$$

29

$$G_\gamma = -16\pi^{-5/2}\sqrt{\frac{\varepsilon'}{\mu}}\, k^2 \bar{F}_\gamma (ka, \zeta)\,\frac{e^{-i(2kd+\frac{\pi}{4})}}{(kd)^{3/2}}\, \dot{g}^*(\zeta,\zeta) \qquad (39\text{b})$$

where F_ϕ and F_ψ are given by equations (37). Note that Q_ϕ and Q_ψ are determined by the values of the amplitude spectra f and g for one direction α, β only, the direction of vertical incidence $\alpha = 0$, $\beta = 90°$. In other words, only a narrow bundle of elementary plane waves of the incident beam, those travelling in the direction normal to or nearly normal to the wire axis, will significantly contribute to the reciprocity integrals and, hence, to the backscatter power returned to the antenna.

For the example of a Gaussian beam, $f(0,0)$ and $g(0,0)$ are found from equations (15). Inserting these equations into (39) reproduces equations (38) which were obtained by the method of Appendix A for the reciprocity integrals of a wire in the far zone of a Gaussian antenna. Deriving equations (38) by means of the method of stationary phase has the advantage that no restrictions have to be imposed on γ_y or γ_z. These equations, therefore, hold for small as well as for large angular deviations of the beam axis from the direction of vertical incidence and the admissible γ_y, γ_z-range is limited only by the approximations which were made in Section 3 to derive the plane wave representation of a Gaussian beam of arbitrary axis direction.

8. BACKSCATTER POWER RETURNED TO ANTENNA WITH GAUSSIAN CHARACTERISTIC

By inserting expressions (33) for Q_ϕ, Q_ψ into equation (7), the ratio of received and transmitted power for a Gaussian antenna illuminating a straight metallic wire is obtained; for N_ϕ, N_ψ we use equations (17). Hence

$$\eta_{\bar{z},\gamma} = \frac{4}{\pi}\,\frac{k\rho^4}{d^3}\,\frac{1}{(1+\bar{\zeta}^2)^{3/2}}\,\bar{F}_{\bar{z},\psi}(ka,\bar{\zeta})\,\bar{F}^*_{\bar{z},\gamma}(ka,\bar{\zeta})\,\times \qquad (40)$$

$$\times\,\frac{\exp\left\{-2(k\rho_0)^2\left[\operatorname{ctg}^2\gamma_z + \frac{\operatorname{ctg}^2\gamma_y}{1+\bar{\zeta}^2}(1+q(\operatorname{ctg}^2\gamma_y))\right]\right\}}{\sin^4\gamma_y\,\sin^4\gamma_z\,\rho\rho^*}$$

where $g(\cot g^2 \gamma_j) = -\frac{\tau^2}{(1+\tau^2)^3}(2+5\tau^2+\tau^4)\cot g^2\gamma_j$

$-\frac{\tau^2}{(1+\tau^2)^6}(1+4\tau^2-9\tau^4-16\tau^6-8\tau^8-\tau^{10})\cot g^4\gamma_j \cdots$

(40)

and $p(\gamma_j,\gamma_z)p^*(\gamma_j,\gamma_z) = 1+\frac{\tau^2}{1+\tau^2}(\cot g^2\gamma_z +2(1-\frac{\tau}{4}\frac{1-3\tau^2}{(1+\tau^2)^2})\cot g^2\gamma_j)\cdots$

≈ 1

with $\tau = \frac{k\rho_0^2}{d}$

Equations (40) hold for a wire in the Fresnel region as well as for a wire in the far field region of the antenna. In the former case, τ is in the order of or greater than unity; in the latter case, τ is small compared to unity so that equation (40) can be simplified to:

$$\hat\eta_{z,\gamma} = \frac{4}{\pi}\frac{k\rho_0^4}{d^3}\bar F_{z,\gamma}(ka,0)\bar F_{z,\gamma}^*(ka,0)\frac{exp\{-2(k\rho_0)^2(\cot g^2\gamma_z+\cot g^2\gamma_j)\}}{\sin^4\gamma_j \sin^4\gamma_z}$$

(41)

for $\tau \ll 1$

In either case, the power ratio η is at a maximum for vertical incidence - if the beam axis intersects the wire axis at right angles - and decreases exponentially as the beam axis is turned away from this direction of incidence. No side lobes are encountered for a Gaussian antenna, at least not in the interesting range of small angular deviations from vertical incidence where η has appreciable values. Note that the dependence of η on the antenna axis angle γ_z is the same for a wire in the Fresnel and in the far field region, while dependence on the axis angle γ_y varies with d. In other words, turning of the beam axis in the plane containing the wire axis leads to a variation in η which is essentially independent of the distance between antenna and wire. Turning of the beam axis in the plane normal to the wire axis, on the other hand, produces a variation in η which becomes less and less rapid as

31

the spacing between antenna and wire is decreased.

The dependence of η on distance d between antenna and wire for vertical incidence (γ_y, $\gamma_z = 90^o$) is given by

$$\eta_{\bar{\varphi},\varphi} \sim (kd \cdot \sqrt{1 + \bar{\varepsilon}^2})^{-3} = \{(kd)^2 + (k\rho)^4\}^{-\frac{3}{2}} \tag{42}$$

$$for \quad \gamma_y \cdot \gamma_z = 90^o$$

Hence $\eta = \eta(d)$ remains essentially constant near the antenna ($\tau \gg 1$); and in the far zone ($\tau \ll 1$), decreases with d^{-3}. The deviation from the usual d^{-4} dependence in this region is due to the fact that the scatter object in this case is a wire infinitely extended in one dimension. In the preceding section we saw that only a narrow bundle of elementary plane waves of the incident beam contributes significantly to the radar response of a long wire situated in the far field region of the antenna. The directions of propagation of these elementary waves form a small solid angle about the direction of vertical incidence $\alpha = 0$, $\beta = 90^o$. We denote this solid angle by $\Delta\Omega = \Delta\alpha \, \Delta\beta$, where $\Delta\alpha$ is the angular width of the wave bundle in the plane perpendicular to the wire axis and $\Delta\beta$ is the angular width in the plane containing the wire axis. The method of stationary phase by which this result was derived shows furthermore that $\Delta\Omega$ becomes smaller and smaller as distance d between antenna and wire is increased. We have $\Delta\Omega \sim 1/d$ and hence

$$\Delta\alpha, \, \Delta\beta \sim \frac{1}{\sqrt{d}}$$

The portion of the wire lying within the solid angle $\Delta\Omega$ can be termed the "effective length" of the wire, since this portion essentially determines the backscatter field received by the antenna. The effective length is obviously given by $\ell = d\Delta\beta$ and consequently increases with $\sqrt{d}$; its contribution to the field strength of the scatter field near the antenna is proportional to

$$\bar{E}_{sc} \sim \frac{\bar{E}_{in} \ell}{\ell} \sim \frac{1}{d^{3/2}}$$

where

$$E_{in} \sim \frac{1}{d}$$

32

denotes the incident field strength at the wire. The received backscatter power is obviously proportional to $E_{sc}E_{sc}^{*}$ and, hence, $\eta \sim d^{-3}$ in accordance with relation ( ).

The dependence of η on wire radius a is determined by the functions $F_{\phi}(ka,\tau)$ and $F_{\psi}(ka,\tau)$, equations (34). For sufficiently thin wires which satisfy condition (— when the wire is situated in the far field region of the antenna this condition is satisfied for all wire radii — these functions can be approximated by $F_{\phi}(ka,0)$ and $F_{\psi}(ka,0)$ as given by equations (37). In Figs. 5 and 6. the amplitude and phase of the latter functions are plotted for the range $0 \leq ka \leq 15$. For small ka, F_{ϕ} and F_{ψ} differ substantially.

This has to be expected as the backscatter properties of thin wires depend strongly on the polarization of the incident field. A field derived from the electric vector potential ϕ comprises a strong electric field component parallel to the wire axis. The ratio of scattered to incident power for this type field therefore will be substantially higher than for a field derived from the magnetic vector potential ψ, which contains only electric field strength components normal to the wire axis. In both cases, of course, the scattered power approaches zero if $ka \to 0$.

A series expansion for small ka yields

$$\bar{F}_{\phi}(ka,0) \approx -\frac{1}{1-i\frac{2}{\pi}\ln(\frac{cka}{2})} \quad , \qquad \bar{F}_{\psi}(ka,0) \approx -i\frac{3}{4}\pi(ka)^2 \qquad (43)$$

$$for\ ka < 0.5$$

where $\ln c = 0.5772\ldots$ is the Eulerian constant. Hence, for small ka the received backscatter power varies with $[\ln ka]^{-2}$ for fields derived from the electric vector potential, but with $(ka)^4$ for fields derived from the magnetic vector potential.

With increasing wire radius, the dependence of η on polarization of the incident field diminishes. In the range where the wire diameter is in the order of one wavelength, F_{ϕ} increases monotonically with ka, while F_{ψ} shows "ripples" whose amplitudes decrease with increasing ka. For sufficiently thick wires ($ka > 10$), the functions F_{ϕ} and F_{ψ} approach each other. An asymptotic expansion yields:

$$\bar{F}_{\phi}(ka,0) \approx \bar{F}_{\psi}(ka,0) \approx \frac{1}{2}\sqrt{\pi ka}\, e^{i(2ka-\frac{5}{4}\pi)} \qquad (44)$$
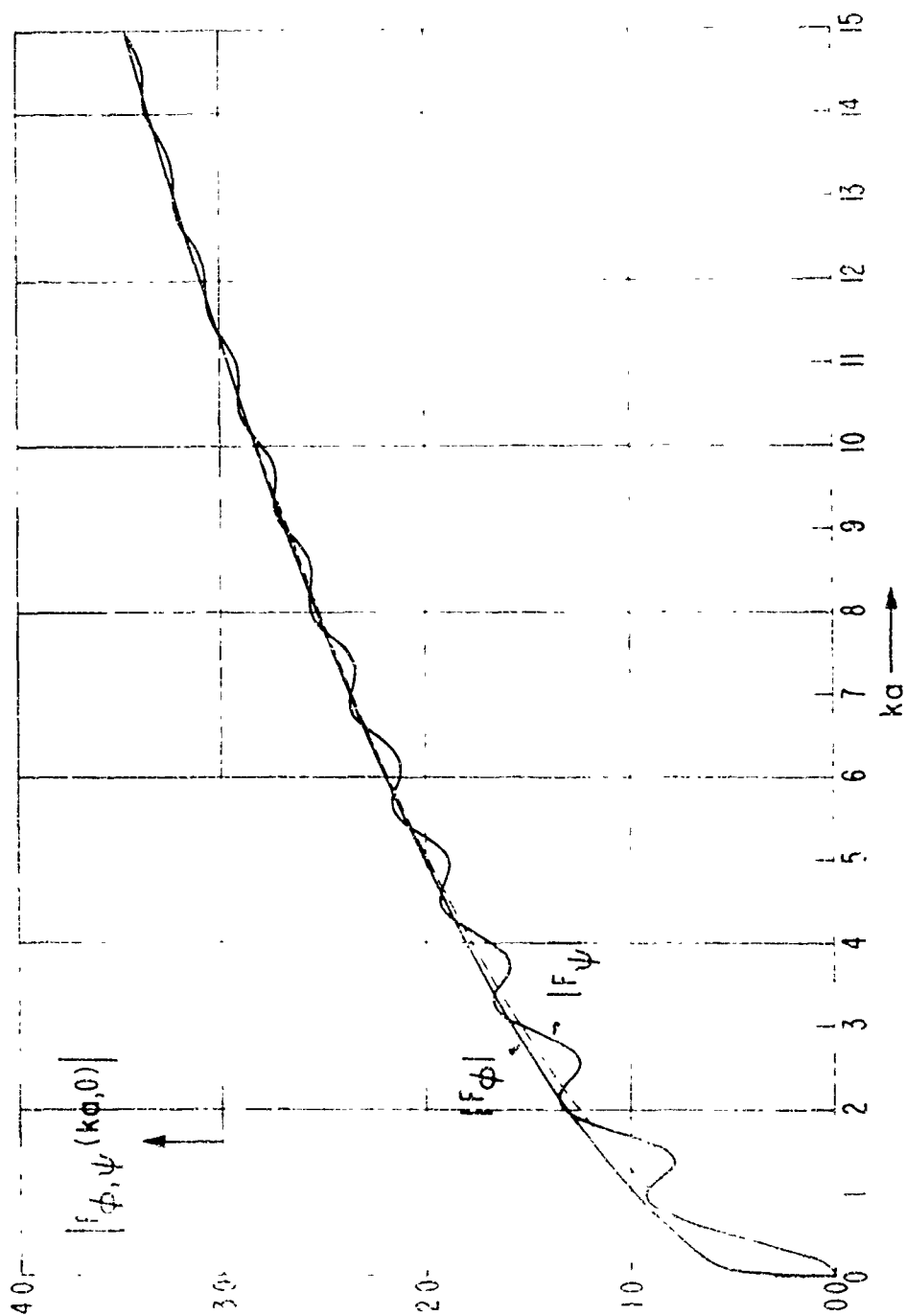
$$for\ ka > 10$$

FIG. 5. Amplitudes of functions $F_\phi(ka, 0)$ and $F_\psi(ka, 0)$ plotted versus ka. The dotted curve indicates the asymptotic amplitude $1/2\sqrt{\pi ka}$. For ka > 8, the amplitude of F_ϕ is in good agreement with the asymptotic curve while the amplitude of F_ψ still oscillates noticeably about this curve.
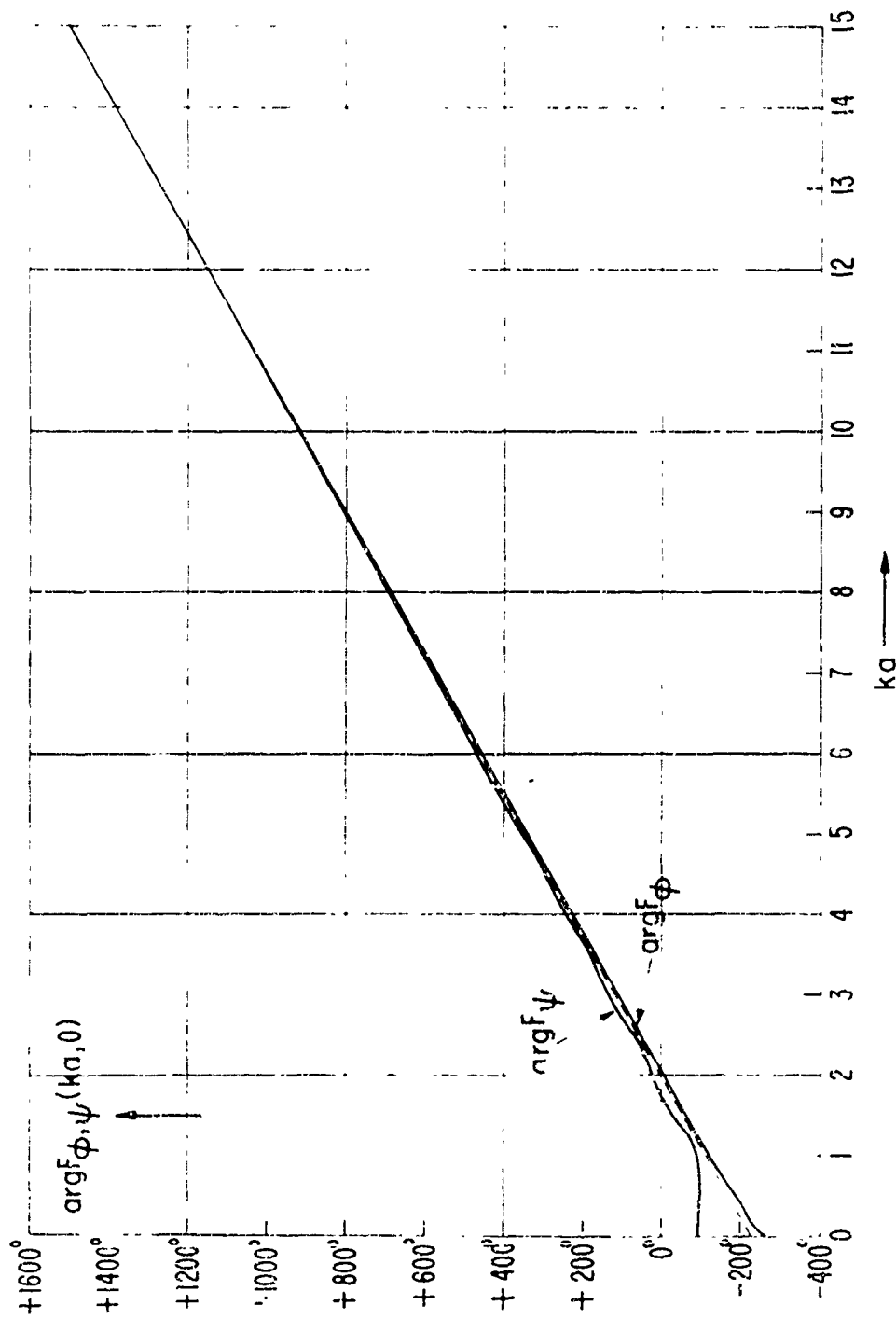
FIG. 6. Phase of functions $F_\phi(ka, 0)$ and $F_\psi(ka, 0)$ plotted versus ka. The dotted curve indicates the asymptotic phase $2ka - 5\pi/4$. For $ka > 6$, the phases of F_ϕ and F_ψ are in good agreement with the asymptotic curve; $\arg F_\phi$ is slightly below and $\arg F_\psi$ slightly above $2ka - 5\pi/4$.

35

and the received backscatter power increases linearly with ka in both cases.

In the interesting range of small deviations of γ_y, γ_z from 90°, the incident beam derived from the electric vector potential is polarized nearly parallel to the wire axis; the incident beam derived from the magnetic vector potential is polarized normal to the wire axis (see Eqs. (13) and (14)). Expressions (40) for η_ϕ and η_ψ accordingly yield the ratio of received to transmitted power for these two directions of polarization. If the polarization direction of the incident beam forms an angle θ with the wire axis other than 0 or 90°, the beam is described by superposition of two fields derived from an electric and a magnetic vector potential

$$\hat{\vec{\Phi}}_p = \vec{\Phi}_p \cos\theta \quad and \quad \hat{\vec{\psi}}_p = \vec{\psi}_p \sin\theta$$

respectively where the distribution of $\phi_p = \psi_p$ in the antenna plane x = -d is, as before, given by equation (14). The power ratio $\eta = \eta(\theta)$ in this case is still described by the right-hand side of equation (40) if we replace the function $F_{\phi,\psi}(ka,\tau)$ by

$$F(ka,\tau;\theta) = F_{\phi}(ka,\tau)\cos^2\theta + F_{\psi}(ka,\tau)\sin^2\theta \tag{45}$$

This result is obtained by modifying expressions (31) and (32) for Q_ϕ, Q_ψ and expressions (17) for N_ϕ, N_ψ by appropriate factors $\cos^2\theta$ and $\sin^2\theta$, and by inserting the modified expressions into equation (7). One merely has to observe that fields derived from the electric and magnetic vector potentials do not interact in regard to Q or N.

9. GENERAL SOLUTION OF RADAR PROBLEM FOR WIRE IN FAR FIELD REGION OF ANTENNA

If the wire is located in the far zone of the antenna, a general expression for the power ratio η can be derived which holds for any antenna characteristic. By inserting Q_ϕ and Q_ψ in the general form of equations (39) into equation (7), we obtain:

$$\eta = 67 \ldots \frac{}{(F_\phi + F_\psi)^2} \tag{46}$$

$$\ldots \{ \ldots F_{\phi}(ka,\zeta)F_{\phi}^*(ka,\zeta) + [y(\zeta) \cdot \eta^*(\zeta,\zeta)]^2 F_{\psi}(ka,\zeta)F_{\psi}^*(ka,\zeta)$$

$$\ldots [y(\zeta) \cdot f^*(\zeta,\zeta)]^2 F_{\phi}(ka,\zeta)F_{\psi}^*(ka,\zeta) + [y(\zeta) \cdot f^*(\zeta,\zeta)]^2 F_{\psi}(ka,\zeta)F_{\phi}^*(ka,\zeta) \}$$

36

where $F_\phi(ka,0)$ and $F_\psi(ka,0)$ are defined by equations (37) and plotted in Figures 5 and 6. N_ϕ and N_ψ can be expressed in terms of the amplitude spectra f and g according to equations (16). Both vector potentials, Φ_p and Ψ_p, are in general required for description of the field of an antenna.

The amplitudes $f(0,0)$ and $g(0,0)$ can be related to the value of the radiation characteristic of the antenna for the direction normal to the wire axis. In an obvious generalization of the definition of the directivity gain, we describe the radiation characteristic of the antenna by the gain function

$$G = \frac{4\pi r^2 S_t}{N_t} \tag{47}$$

where S_t is the radial component of the Poynting vector in the far zone of the unperturbed antenna field, $N_t = N_\phi + N_\psi$ is the total radiated power, and $r = \{(x + d)^2 + y^2 + z^2\}^{\frac{1}{2}}$ is the radial distance from the center of the antenna aperture (see Fig. 2); kr, of course, is assumed to be a large number. The electric and magnetic field components in the far field region of the antenna can be determined by an asymptotic evaluation of equations (10) in connection with equations (9). For the direction of vertical incidence which we shall indicate by the superscript (x), we obtain

$$E_x^{(x)} = 0 \qquad\qquad \sqrt{\frac{\mu}{\varepsilon}}\, H_x^{(x)} = 0$$

$$E_y^{(x)} = +g(0,0)\,U(r) \qquad\qquad \sqrt{\frac{\mu}{\varepsilon}}\, H_y^{(x)} = -f(0,0)\,U(r) \tag{48}$$

$$E_z^{(x)} = +f(0,0)\,U(r) \qquad\qquad \sqrt{\frac{\mu}{\varepsilon}}\, H_z^{(x)} = +g(0,0)\,U(r)$$

$$\text{where}\quad U(r) = 2\pi k\,\frac{e^{-ikr}}{r}$$

and consequently

$$S_t^{(x)} = 4\pi^2\, \frac{k^2}{r^2} \sqrt{\frac{\varepsilon}{\mu}}\, [\, f(0,0) f^*(0,0) + g(0,0) g^*(0,0)\,] \tag{49}$$

37

The partial fields derived from the electric and magnetic vector potentials apparently yield asymptotic electric field strengths which, for the direction of vertical incidence, are tangential and normal to the wire axis, respectively. The phases of the two partial fields will in general be different with the result that the total asymptotic field will be elliptically polarized. We introduce a polarization angle $\Theta^{(x)}$ for the direction of vertical incidence by writing:

$$E_y^{(x)} = E^{(x)} \sin \Theta^{(x)} , \qquad E_z = E^{(x)} e^{i \zeta^{(x)}} \cos \Theta^{(x)} \tag{50}$$

where $\zeta^{(x)}$ is the phase difference between $E_y^{(x)}$ and $E_z^{(x)}$, and
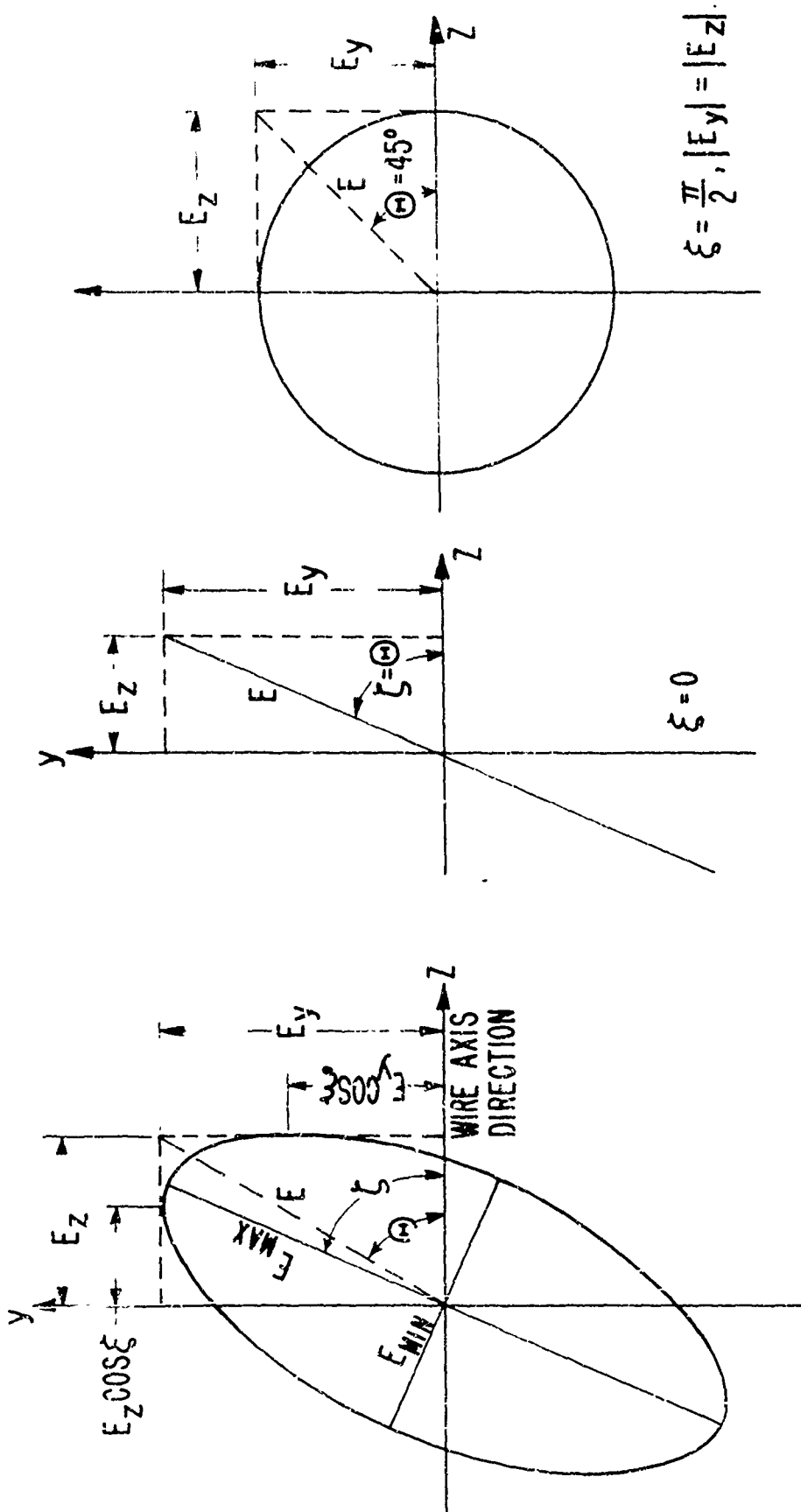
$$|E^{(x)}| = \left\{ E_y^{(x)} E_y^{(x)*} + E_z^{(x)} E_z^{(x)*} \right\}^{\frac{1}{2}} , \qquad \arg E^{(x)} = \arg E_y^{(x)}$$

The meaning of $E^{(x)}$, $\Theta^{(x)}$, and $\zeta^{(x)}$ is illustrated by Fig. 7 where a polarization ellipse and its special cases are shown. (The superscript (x) has been omitted in this figure.) In the case of linear polarization, ζ is zero, E is the total incident field strength, and Θ is the polarization angle measured against the wire axis. Circular polarization is characterized by $\zeta = +90^\circ$ and $\Theta = \pm 45^\circ$; the actual field strength is $E/\sqrt{2}$. In the general case of elliptic polarization, Θ and ζ are related to the angle ζ which the major axis of the polarization ellipse forms with the wire axis and to the axial ratio $\varkappa = E_{min}/E_{max}$ according to

$$\operatorname{tg} \Theta = \left\{ \frac{\varkappa^2 + \operatorname{tg}^2 \zeta}{1 + \varkappa^2 \operatorname{tg}^2 \zeta} \right\}^{\frac{1}{2}} , \qquad \cot \zeta = \frac{1 - \varkappa^2}{2\varkappa} \sin 2\zeta$$

With equations (47) to (50), we can now express the products ff^*, gg^*, and fg^* at $\alpha = 0$, $\beta = 90^\circ$ in terms of $G^{(x)}$, $\Theta^{(x)}$, and $\zeta^{(x)}$

$$f(0,0) f^*(0,0) = \frac{1}{k r^3} \sqrt{\frac{\mu}{\varepsilon}} \frac{1}{k^2} N_f \zeta^{(x)} \cos^2 \Theta^{(x)} \tag{51a}$$

FIG. 7. Polarization ellipse and special cases for field incident in direction normal to wire axis. The direction of incidence is the x-axis; the wire axis coincides with the z-axis.

39

$$g(0,0)\,g^{*}(0,0) = \frac{1}{16\,\pi^3}\sqrt{\frac{\mu}{\varepsilon}}\ \frac{1}{k^2}\ \mathcal{N}_c\,\mathcal{G}^{(x)}\sin^2\Theta^{(x)} \tag{51b}$$

$$f(0,0)\,g^{*}(0,0) = \frac{1}{16\,\pi^3}\sqrt{\frac{\mu}{\varepsilon}}\ \frac{1}{k^2}\ \mathcal{N}_c\,\mathcal{G}^{(x)}\,e^{i\xi^{(x)}}\cos\Theta^{(x)}\sin\Theta^{(x)} \tag{51c}$$

By inserting these expressions into equation (46), we finally obtain

$$\eta = \frac{1}{4\pi}\ \frac{\mathcal{G}^{(x)2}}{(kd)^3}\left|\ F_{\Phi}(ka,0)\,e^{+i\xi^{(x)}}\cos^2\Theta^{(x)} + F_{\psi}(ka,0)\,e^{-i\xi^{(x)}}\sin^2\Theta^{(x)}\right|^2 \tag{52}$$

Since η is determined by the value of the radiation characteristic of the antenna for only one direction - the direction normal to the wire axis - only the power transmitted by the antenna in this direction will significantly contribute to the energy which is returned to and received by the antenna after scattering at the wire. The received backscatter power depends on the polarization properties of the antenna far field. This dependence obviously stems from the fact that the backscatter properties of a straight wire are different for incident fields polarized parallel to and normal to the wire axis. If the radiation characteristic and the polarization properties of the far field of a given antenna are known, equation (52) permits determination of the ratio of received to transmitted power for any orientation of the antenna in respect to the wire. One merely has to insert into equation (52) the values of G, Θ, and ξ which are associated in each case with the directions normal to the wire axis. We discuss three special cases:

(1) If equation (52) is applied to the example of a Gaussian antenna, one should obtain equation (41), which is indeed the case. This is evident if one considers that, for a Gaussian antenna (as characterized by equations (13)) the value of $G^{(x)}$ becomes:

$$\mathcal{G}^{(x)} = \frac{4\,(k\gamma_0)^2}{\sin^2\gamma_y\,\sin^2\gamma_z}\ \exp\left\{-(k\gamma_0)^2(\cot g^2\gamma_y + \cot g^2\gamma_z)\right\}$$

Equation (52), however, leads to a more general expression for η insofar as this expression applies to linearly as well as elliptically polarized incident fields while equation (41), even if generalized according to equation (45), is limited to linear polarization.

(2) The right-hand side of equation (52) has a particularly simple form when the incident field is linearly polarized and the wire radius is so large (ka > 10) that F_ϕ and F_ψ can be replaced by their asymptotic representations (44). Since in the asymptotic range these two functions do not differ, η becomes independent of the polarization direction of the incident field:

$$ \eta = \frac{1}{16} \frac{ka}{J_o(\omega)} , \; G^{(x)^2} \tag{53} $$

Hence, measuring η while turning the antenna yields the radiation characteristic of the antenna or, more precisely, the square of the gain function G.

(3) The right-hand side of equation (52) becomes zero if

$$ tg^2 \Theta^{(x)} = \left| \frac{\overline{F_\phi}(ka,0)}{\overline{F_\psi}(ka,0)} \right| \quad and \quad 2\xi^{(x)} = \pm \pi - (arg\, \overline{F_\phi}(ka,0) - arg\, \overline{F_\psi}(ka,0)) \tag{54} $$

For sufficiently thick wires (ka > 10), the functions F_ϕ and F_ψ do not appreciably differ and requirements (54) reduce to

$$ \Theta^{(x)} = \pm \frac{\pi}{4} , \qquad \xi^{(x)} = \pm \frac{\pi}{2} \tag{55} $$

i.e. to the conditions for circular polarization of the incident field. The explanation in this case is obvious: if $F_\phi = F_\psi$, the backscatter properties of the wire are the same for fields polarized tangential to and normal to the wire axis so that an incident field which for the direction vertical to the wire axis is circularly polarized will lead to a backscatter field which is also circularly polarized with the same direction of rotation, but the opposite direction of propagation. Seen in their respective directions of propagation, the two fields, therefore, rotate in opposite directions and an antenna emitting the incident field cannot receive the backscatter field.

Actually η will not become zero, but will be very small since the antenna will still receive backscatter power from directions of incidence other than 90°. Mathematically speaking, the right-hand side of equation (52)

41

is the first term of an asymptotic expansion of the power ratio η for large kd. If this term is zero, η is determined by the second asymptotic term which decreases with $(kd)^{-4}$ as opposed to the $(kd)^{-3}$ dependence of the first term. Since kd is supposed to be a large number, the received backscatter power will decrease rapidly as conditions (55) are approached.

These considerations imply that the receiving antenna is identical with the transmitting antenna. If the receiving and transmitting antennas on the other hand are matched to circularly polarized fields with opposite directions of rotation, the full available backscatter power will be received and η, as in the case of linear polarization, is given by equation (53).

10. RADAR CROSS SECTION OF STRAIGHT METALLIC WIRE

We saw in the last section that the radar response of an infinitely long wire situated in the far field region of the illuminating antenna, is determined by the value of the radiation characteristic of the antenna for the direction of vertical incidence only. Hence the wire can in principle be replaced by a finitely bounded scatter object with an appropriate radar cross section placed at the point where the direction of vertical incidence intersects the wire axis. Comparison of equation (52) with the well-known radar range equation:

$$ \eta = \frac{N_r}{N_t} = \frac{\lambda^2}{(4\Gamma)^3} \frac{G^2}{d^4} \sigma \tag{56} $$

where G is the value of the antenna gain function for the direction under which the antenna sees the scatter object, immediately yields for the equivalent radar cross section

$$ \sigma = \frac{4d}{k} \left| \overline{F}_{\phi}(ka,0) e^{i\xi^{(n)}} \cos^2\Theta^{(x)} + \overline{F}_{\vartheta}(ka,0) e^{-i\xi^{(x)}} \sin^2\Theta^{(x)} \right|^2 \tag{57} $$

and we obtain in particular for the case of a linearly polarized incident field if the direction of polarization at vertical incidence is parallel to the wire axis $(\hat{\vartheta}^{(x)} = 0)$

$$ \sigma_{\parallel} = \frac{4d}{k} \overline{F}_{\phi}(ka,0) \overline{F}_{\phi}^{*}(ka,0) \tag{58a} $$

42

and if the direction of polarization is normal to the wire axis $(\theta^{(x)} = 90^{o})$

$$\sigma_{\perp} = \frac{4\ell}{k} \, \bar{F}_{\psi}(k\alpha, \zeta) \cdot \bar{F}_{\psi}^{r}(k\alpha, \zeta) \tag{58b}$$

For sufficiently thick wires (ka > 10), F_{ϕ} and F_{ψ} can be approximated by their asymptotic representations (44), and equations (58) reduce to

$$\sigma_{\parallel} \approx \sigma_{\perp} \approx rad$$

The radar cross section of a long wire according to these equations increases linearly with distance d between antenna and wire. This is consistent with the earlier obtained result that the "effective length" of the wire, i.e., the portion of the wire which significantly contributes to the backscatter field near the antenna increases with $\sqrt{d}$. Since the quantity proportional to the effective length ℓ is the received field strength and the quantity proportional to the radar cross section σ is the received power, we have $\sigma \sim \ell^2$ where both σ and ℓ^2 are proportional to d.

11. CONCLUSIONS

The scatter field and radar response of an infinitely long straight metallic wire have been derived under the assumption that the source of excitation is an antenna radiating a Gaussian beam of narrow beam width in the order of 1°. Two cases can be distinguished, that the wire crosses the Fresnel region (near field region) of the antenna and that the wire is situated in the far field region of the antenna. In the former case, the theory is limited to wire radii a < ρ_0 where ρ_0 is the beam radius at the antenna; in the latter case, wires of arbitrary diameters are admissable. The following results have been obtained:

(1) The scatter field produced by diffraction of the incident beam at the wire has essentially the same distribution in every plane through the wire axis; it differs from plane to plane only by an amplitude factor. If the wire is located in the far field region of the antenna, the scatter field is concentrated near a conical surface (about the wire axis) whose aperture angle is equal to the angle which the axis of the incident beam incloses with the direction of the wire axis.

(2) The fraction η of the radiated power which after scattering at the wire is returned to and received by the antenna is at a maximum for vertical incidence - when the beam axis intersects the wire axis at right angles - and decreases exponentially as the beam axis is turned away from the direction of incidence; no side lobes are encountered in case of Gaussian illumination, at least not in the interesting range of small angular deviations (< 15°) from vertical incidence where η has appreciable values.

(3) The expression derived for the radar response of a wire situated in the far field region of the illuminating antenna can be generalized so that it holds for any antenna characteristic. This generalization shows that η is proportional to the square of the value of the radiation characteristic of the antenna for the direction intersecting the wire axis at right angles. In other words, only the energy radiated by the antenna in the direction of vertical incidence will contribute significantly to the backscatter power returned to the antenna. A consequence of this result is that a radar cross section can be assigned to the wire, even though it is assumed to be infinitely long. This radar cross section increases linearly with distance between antenna and wire.

(4) The radar response of a wire in the far field region of the antenna decreases with the inverse third power of distance d between antenna and wire. The deviation from the usual d^{-4} relation is due to the fact that the scatter object, the wire, is infinitely extended in one dimension. If the wire crosses the Fresnel region of the antenna (and the antenna radiates a Gaussian beam) the radar response for vertical incidence decreases with distance d according to

$$\eta = \{(kd)^2 + (k\rho_0)^4\}^{-\frac{3}{2}}$$

where ρ_0 is the beam radius at the antenna.

(5) The dependence of the radar response η on wire radius a is essentially the same for a wire crossing the Fresnel region and for a wire situated in the far field region of the antenna. The received backscatter power in general increases with a, and for thin wires (ka < 1) shows a marked dependence on the polarization of the incident field. An incident beam polarized parallel to the wire axis produces a substantially stronger response than an incident beam polarized normal to the wire axis. With increasing wire radius, the dependence of η on polarization diminishes and practically disappears when ka $\approx$ 10. For ka > 10, the radar response increases linearly with a for either polarization.

The theory was derived assuming that the incident beam, and therefore also the field scattered by the wire, are strictly time harmonic. The results consequently hold for CW-radar systems, but can be applied also to radar systems employing pulsed fields provided the frequency spectrum of the pulses is sufficiently narrow. The quantities kd and $(k\rho_0)^2$ can then be treated as constants and the expressions derived for η under the assumption of time harmonic field will be valid approximations for the ratio of received to transmitted energy per pulse.

LITERATURE CITED

[1] J. H. Van Vleck, F. Block, M. Hamermesh, Theory of radar reflections from wires or thin metallic strips, J. Appl. Phys., Vol. 18, pp. 274-294, 1947.

[2] C. H. Papas, Diffraction by a cylindrical obstacle, J. Appl. Phys., Vol. 21, pp. 318-325, April 1950.

[3] F. E. Borgnis, C. H. Papas, Randwertprobleme der Mikrowellenphysik, Springer-Verlag, Berlin, 1955.

[4] Special Issue on Radar Reflectivity, Proceedings IEEE, Vol. 53, August 1965:

 M. G. Andreasen, Scattering from cylinders with arbitrary surface impedance, pp. 812-817.

 J. W. Crispin, A. L. Maffett, Radar cross section estimation for simple shapes, pp. 833-848.

 H. A. Corriher, B. O. Pyron, A bibliography of articles on radar reflectivity and related subjects, pp. 1025-1058; see in particular Section 19, "Cylinders," pp. 1035-1036.

[5] H. Y. Yee, Scattering of electromagnetic waves by circular dielectric coated conducting cylinders with arbitrary cross section, IEEE Trans. on Antennas and Prop., Vol. AP-13, pp. 822-823, Sept. 1965.

[6] C. R. Mullin, R. Sandburg, C. O. Velline, A numerical technique for the determination of scattering cross section of infinite cylinders of arbitrary geometrical cross section, IEEE Trans. Antennas and Prop., Vol. AP-13, pp. 141-149, January 1965.

[7] V. J. DiCaudio, W. W. Martin, Approximate solution to bistatic radar cross section of finite length, infinitely conducting cylinder, IEEE Trans. on Antennas and Prop., Vol. AP-14, pp. 668-669, September 1966.

[8] J. H. Richmond, TE-wave scattering by a dielectric cylinder of arbitrary cross section shape, IEEE Trans. on Antennas and Prop., Vol. AP-14, pp. 460-464, July 1966.

[9] J. H. Richmond, Scattering by imperfectly conducting wires, IEEE Trans. on Antennas and Prop., Vol. AP-15, pp. 802-806, Nov. 1967.

[10] R. Harrington, Matrix methods for field problems, Proc. IEEE, Vol. 55, pp. 136-149, February 1967.

[11] A. Mayer, Mean radar cross section of finite cylindrical wires: Dependence on conductivity and frequency, Proc. IEEE, Vol. 55, pp. 1502-1504, August 1967.

[12] W. S. Lucke, Electric dipoles in the presence of elliptic and circular cylinders, J. Appl. Phys., Vol. 22, pp. 14-19, January 1951.

[13] G. N. Tsandoulas, Scattering of a dipole field by finitely conducting and dielectric circular cylinders, IEEE Trans. on Antennas and Prop., Vol. AP-16, pp. 324-328, May 1968.

[14] J. R. Christian, G. Goubau, J. W. Mink, and F. Schwering, Diffractional field distortion and cross-coupling in guided optical multibeam transmission (To be published).

[15] G. Goubau, Optical relations for coherent wave beams, Proceedings of Symposium on Electromagnetic Theory and Antennas, pp. 907-918, Copenhagen, 1962, Pergamon Press.

[16] G. Goubau, F. Schwering, Electromagnetic fields in a halfspace free of sources, USASRDL Technical Report 2293, February 1962.

[17] W. Magnus, F. Oberhettinger, Formulas and Theorem for the Functions of Mathematical Physics, p. 18, Chelsea Publishing Co., New York, 1954.

APPENDIX A

APPROXIMATE EVALUATION OF THE RECIPROCITY INTEGRALS Q_ϕ AND Q_ψ (Gaussian Illumination)

We evaluate the reciprocity integrals Q_ϕ and Q_ψ, equations (31). The evaluation procedure uses approximations based on the three following assumptions:

(1) The beam width of the incident Gaussian beam is in the order of 1°. This means $k\rho_0$ is in the order of 100. The quantity kd is in the order of $(k\rho_0)^2$ when the wire crosses the Fresnel region of the antenna, and is large compared to $(k\rho_0)^2$ when the wire is situated in the antenna far zone.

(2) The wire radius does not exceed the value

$$a_{Max} = \rho_0 \left(1 + \left(\frac{d}{k\rho_0^2} \right)^2 \right)^{\frac{1}{4}} \tag{A.1}$$

The summation over m in the integrand of equations (31) can then be limited to terms with $|m| < 2[(k\rho_0)^4 + (kd)^2]^{\frac{1}{4}}$, this means to terms varying with α, α', β slowly as compared to the exponential part of the integrand. The condition $a < a_{max}$ does not impose a severe restriction. For a wire crossing the Fresnel region of the antenna, this condition essentially requires $a < \rho_0$; therefore wire diameters of several wavelengths are admissible. The diameter of a wire in the antenna far zone is practically not limited by this condition.

(3) The beam axis angles γ_y and γ_z are close to 90°; their deviations from this value do not exceed 15°. We may restrict ourselves to considering a small γ_y, γ_z-range as Q_ϕ and Q_ψ decrease rapidly with increasing deviations of γ_y and γ_z from 90°, and for a deviation of 15° already are exceedingly small (see equation (A.14)).

Substituting in equations (31)

$$\sin\alpha = u, \quad \sin\alpha' = v, \quad \cos\beta = w \tag{A.2}$$

we write

$$Q_{\xi,\psi} = \frac{2}{\pi} \sqrt{\frac{\varepsilon}{\mu}} \, k^6 \rho_0^4 \, \frac{e^{-(k\rho)^2 \cot g^2 \gamma_2}}{\sin^2 \gamma_1 \sin^4 \gamma_2} \times$$

$$\times \sum_{m=-\infty}^{\infty} \iiint_{u,v,w=-1}^{+1} \overline{H}_{\xi,\psi}^{(m)}(u,v,w) \, e^{+\mu_m(u,v,w)} \, du \, dv \, dw$$

(A.3)

where

$$\mu_m(u,v,w) = -ikd\left(\sqrt{1-u^2} + \sqrt{1-v^2}\right)\sqrt{1-w^2} - im(u-v)$$

$$-\frac{1}{2}(k\rho_0)^2 \left[\left(\frac{u\sqrt{1-w^2}-\cos\gamma_1}{\sin\gamma_1}\right)^2 + \left(\frac{v\sqrt{1-w^2}-\cos\gamma_1}{\sin\gamma_1}\right)^2 + \frac{2w^2}{\sin^2\gamma_2} \right]$$

$$\overline{H}_{\xi}^{(m)}(u,v,w) = (-1)^{m+1} \frac{\overline{J}_m\left(ka\sqrt{1-w^2}\right)}{H_m^{(2)}\left(ka\sqrt{1-w^2}\right)} (1-w^2)^2 .$$

(A.4)

$$\times \exp\left\{+im\left[(u-\arcsin u)-(v-\arcsin v)\right]\right\}$$

$$\overline{H}_{\psi}^{(m)}(u,v,w) = (-1)^m \frac{\overline{J}_m'\left(ka\sqrt{1-w^2}\right)}{H_m^{(2)'}\left(ka\sqrt{1-w^2}\right)} (1-w^2)^2 .$$

$$\times \exp\left\{+im\left[(u-\arcsin u)-(v-\arcsin v)\right]\right\}$$

Since kd and $(k\rho_0)^2$ are large numbers, the exponential functions $e^{+\mu_m(u,v,w)}$ in the integrands of equation (A.3) change rapidly with u,v,w

while the functions $A_{\vartheta,\psi}^{\pm}$ vary only moderately. To evaluate the integrals, we use a method which is in essence the method of steepest descent.

Differentiation with regard to u, v, w shows that the exponent $\mu_m(u,v,w)$ becomes stationary at the point

$$u = u_m \, , \qquad v = v_m \, , \qquad w = c \tag{A.5}$$

where u_m and v_m are solutions of the (fourth order) equations

$$u_m \left(1 + \frac{\sin^2 \gamma_\vartheta}{i\tau \sqrt{1 - u_m^2}} \right) = c_m \, , \qquad v_m \left(1 + \frac{\sin^2 \gamma_\vartheta}{i\tau \sqrt{1 - v_m^2}} \right) = c_m^* \tag{A.6}$$

$$\text{with} \quad c_m = \cos \gamma_\vartheta - \frac{i m}{(k\rho_0)^2} \sin^2 \gamma_\vartheta \, , \qquad \tau = \frac{k \rho_0^2}{d}$$

u_m and v_m have the power series expansions:

$$u_m = b_1 c_m + b_3 c_m^3 + b_5 c_m^5 \ldots \, , \qquad v_m = b_1 c_m^* + b_3 c_m^{*3} + b_5 c_m^{*5} \ldots \tag{A.7}$$

$$\text{with} \quad b_1 = \frac{i\tau'}{1 + i\tau'} \, , \quad b_3 = -\frac{1}{2} \frac{(i\tau')^3}{(1 + i\tau')^4} \, , \quad b_5 = \frac{3}{8} \frac{(i\tau')^5 (1 - i\tau')}{(1 + i\tau')^7}$$

$$\text{and} \quad \tau' = \frac{\tau}{\sin^2 \gamma_\vartheta} \, , \quad \tau = \frac{k \rho_0^2}{d}$$

For kd $\ll (k\rho_0)^2$ and kd $\gg (k\rho_0)^2$, u_m and v_m approach real values. In the first case, $u_m = v_m = \cot g \, \gamma_y$; and in the second case, $u_m = v_m \to 0$. In the intermediate kd-range, u_m and v_m are complex; their real parts lie between 0 and $\cot g \, \gamma_y$, and their imaginary parts are small compared to unity.

The paths of integration with regard to u and v are now shifted, as indicated in Fig. 8, so that they transverse the points u = u_m and v = v_m respectively. Thus modified, the range of integration of each summation term in equation (A.3) includes the corresponding stationary point u = u_m, v = v_m, w = 0. Since the exponential functions $e^{+\mu_m(u,v,w)}$ at these points have maximum amplitude and zero phase change and in moving away from these points decrease and oscillate rapidly, only the immediate neighborhood of the points u = u_m, v = v_m, w = 0 will appreciably contribute to the values of the integrals in equation (A.3). In these neighborhoods, the functions $A_1^{(m)}$ and $A_2^{(m)}$ do not vary noticeably, and the exponents μ_m can be replaced by second order approximations[*]

$$\mu_m(u,v,w) \approx \mu_m(u_m,v_m,0) + \frac{1}{2}\left\{ \frac{\partial^2\mu_m}{\partial u^2}\Delta u^2 + \frac{\partial^2\mu_m}{\partial v^2}\Delta v^2 + \frac{\partial^2\mu_m}{\partial w^2}\Delta w^2\right\}_{u_m,v_m,0} \quad (A.8)$$

where

$$\left(\frac{\partial^2\mu_m}{\partial u^2}\right)_{u_m,v_m,0} = + \frac{ikd}{(1-u_m^2)^{3/2}} - \frac{(k\rho_0)^2}{\sin^2\gamma_3}$$

$$\left(\frac{\partial^2\mu_m}{\partial v^2}\right)_{u_m,v_m,0} = + \frac{ikd}{(1-v_m^2)^{3/2}} - \frac{(k\rho_0)^2}{\sin^2\gamma_3} \qquad (A.9)$$

$$\left(\frac{\partial^2\mu_m}{\partial w^2}\right)_{u_m,v_m,0} = + ikd\left(\sqrt{1-u_m^2} + \sqrt{1-v_m^2}\right)$$

$$- (k\rho_0)^2\left[\frac{2}{\sin^2\gamma_2} + \frac{(u_m+v_m)\cos\gamma_3}{\sin^2\gamma_3} - \frac{u_m^2+v_m^2}{\sin^2\gamma_3}\right]$$

and $\Delta u = u-u_m$, $\Delta v = v-v_m$, $\Delta w = w$

---

[*]The mixed second order derivatives $\frac{\partial^2\mu_m}{\partial u\,\partial v}$, $\frac{\partial^2\mu_m}{\partial v\,\partial w}$, $\frac{\partial^2\mu_m}{\partial v\,\partial w}$ are zero at u = u_m, v = v_m, w = 0.
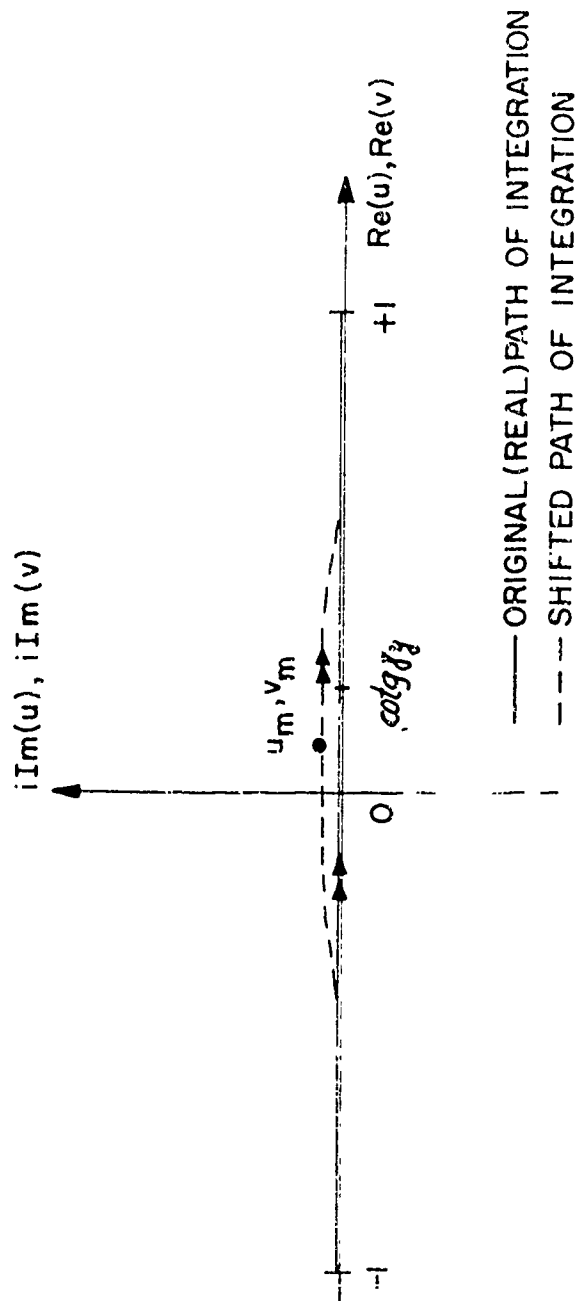
50

FIG. 8. Deformation of paths of integration with regard to u and v from real axes into complex u- and v-planes respectively.

Note that the deformations of the paths of integration in u and v, as indicated in Fig. 8, have been chosen so that Δu and Δv near $u = u_m$ and $v = v_m$ are essentially real. Since the w-integration follows the real axis, Δw, of course, is real.

Extending the range of integration in Δu, Δv, Δw to infinity, which is permissible as no noticeable error is introduced by this modification, the integrations can be carried out in closed form:

$$\iiint_{u,v,w=-1}^{+1} \vec{H}_{\Phi,\Psi}^{(m)}(u,v,w) \, e^{+\mu_m(u,v,w)} \, du\,dv\,dw \;\sim$$

$$\approx \vec{H}_{\Phi,\Psi}^{(m)}(u_m,v_m,0)\, e^{+\mu_m(u_m,v_m,0)}$$

(A.10)

$$\times \iiint_{\Delta u,\Delta v,\Delta w=-\infty}^{+\infty} \exp\left\{ \frac{1}{2}\left[\frac{\partial^2 \mu_m}{\partial u^2}\Delta u^2 + \frac{\partial^2 \mu_m}{\partial v^2}\Delta v^2 + \frac{\partial^2 \mu_m}{\partial w^2}\Delta w^2 \right]_{u_m,v_m,0} \right\} d(\Delta u)\,d(\Delta v)\,d(\Delta w)$$

$$= (2\pi)^{3/2} \vec{H}_{\Phi,\Psi}^{(m)}(u_m,v_m,0)\, \frac{e^{+\mu_m(u_m,v_m,0)}}{\sqrt{-\left(\frac{\partial^2 \mu_m}{\partial u^2}\frac{\partial^2 \mu_m}{\partial v^2}\frac{\partial^2 \mu_m}{\partial w^2}\right)_{u_m,v_m,0}}} \;.$$

and we obtain with equations (A.3), (A.4), and (A.9):

$$Q_{\Phi,\Psi} = 4\sqrt{2\pi}\sqrt{\frac{\varepsilon}{\mu}}\, k^6 f_0^4 \,\times$$

(A.11)

$$\times \sum_{m=-\infty}^{+\infty} \frac{\vec{H}_{\Phi,\Psi}^{(m)}(u_m,v_m,0)}{\sin^2 \psi_1 \sin^4 \psi_2 |\nu^{(m)}(\psi_1,\psi_2)|}\, \exp\left\{ -ikd\left[\sqrt{1-u_m^2} + \sqrt{1-v_m^2}\right] - im(u_m-v_m) \right.$$

$$\left. -\frac{1}{2}(kf_0)^2\left[\left(\frac{u_m-\cos\psi_1}{\sin\psi_1}\right)^2 + \left(\frac{v_m-\cos\psi_1}{\sin\psi_1}\right)^2 + 2\cot^2\psi_2\right] \right\}$$

where

$$p^{(m)}(\gamma_y, \gamma_z) = \left\{ \left[-\frac{ikd}{(1-u_m^2)^{3/2}} + \frac{(k\rho_o)^2}{\sin^2\gamma_y} \right]\left[-\frac{ikd}{(1-v_m^2)^{3/2}} + \frac{(k\rho_o)^2}{\sin^2\gamma_y} \right] \right.$$

$$\left. \cdot \left[-ikd(\sqrt{1-u_m^2} + \sqrt{1-v_m^2}) + ik\rho_o \right]^2 \left(\frac{2}{\sin\gamma_z} + \frac{(u_m+v_m)\cos\gamma_y}{\sin^2\gamma_y} - \frac{u_m^2+v_m^2}{\sin^2\gamma_y} \right) \right\}^{1/2}$$

and

(A.11)

$$\bar{H}_z^{(m)}(u_m, v_m, 0) = (-1)^{n+1} \frac{J_m(ka)}{H_m^{(2)}(ka)} \exp\left\{ +im\left[(u_m - \arcsin u_m) - (v_m - \arcsin v_m) \right] \right\}$$

$$\bar{H}_\gamma^{(m)}(u_m, v_m, 0) = (-1)^m \frac{J_m'(ka)}{H_m^{(2)'}(ka)} \exp\left\{ +im\left[(u_m - \arcsin u_m) - (v_m - \arcsin v_m) \right] \right\}$$

This result can be simplified further. An estimate based on the assumptions stated at the beginning of this appendix shows that the functions $p^{(m)}(\gamma_y, \gamma_z)$ can be replaced by second-order approximations in cotg γ_y and cotg γ_z; the approximate expressions become independent of m:

$$p^{(m)}(\gamma_y, \gamma_z) = \sqrt{2} (-ikd)^{3/2}(1+i\tau)^{3/2} p(\gamma_y, \gamma_z)$$

where $\quad p(\gamma_y, \gamma_z) \sim 1 + \frac{1}{2} \frac{i\tau}{1+i\tau} \left[\cotg^2\gamma_z + 2\left(1 + \frac{7}{4} \frac{i\tau}{(1+i\tau)^2}\right)\cotg^2\gamma_y \right]$

$$\approx 1 \qquad \text{for} \quad \gamma_y, \gamma_z \approx 90^\circ$$

53

In the exponential functions, furthermore, we can approximate

$$-ikd\left[\sqrt{1-u_m^2} + \sqrt{1-v_m^2}\right] - \frac{1}{2}(k\rho_0)^2\left[\left(\frac{u_m-\cos\beta_3}{\sin\beta_3}\right)^2 + \left(\frac{v_m-\cos\beta_3}{\sin\beta_3}\right)^2\right] - im(u_m-v_m)$$

$$\approx -2ikd\sqrt{1-u_0^2} - (k\rho_0)^2\left(\frac{u_0-\cos\beta_3}{\sin\beta_3}\right)^2 + \frac{m^2}{ikd - (k\rho_0)^2}$$

where u_0 ($=v_0$) is the value of u_m and v_m for $m = 0$. Finally, the terms $im(\beta_m - \arcsin u_m)$ and $im(v_m - \arcsin v_m)$ in the exponent of the functions $A_{\Phi,\Psi}^{(m)}$ are small compared to π and therefore can be neglected. Hence

$$Q_{\Phi,\Psi} = 4\sqrt{\pi}\sqrt{\frac{\varepsilon}{\mu}} k^3\rho_0\left(\frac{i\tau}{1+i\tau}\right)^{3/2} \overline{F}_{\Phi,\Psi}(ka,\tau) \cdot$$

$$\cdot \frac{\exp\left\{-2ikd\sqrt{1-u_0^2} - (k\rho_0)^2\left[\left(\frac{u_0-\cos\beta_3}{\sin\beta_3}\right)^2 + \cotg^2\beta_2\right]\right\}}{\sin^2\beta_3 \sin^4\beta_2\, P(\beta_3,\beta_2)}$$

$$(A.12)$$

with

$$u_0 = \frac{i\tau'}{1+i\tau'}\cos\beta_3 - \frac{i}{2}\frac{(i\tau')^3}{(1+i\tau')^4}\cos^3\beta_3 + \frac{3}{8}\frac{(i\tau')^5(1-i\tau')}{(1+i\tau')^7}\cos^5\beta_3 \dots$$

$$\tau' = \frac{\tau}{\sin^2\beta_3}, \qquad \tau = \frac{k\rho_0^2}{d}$$

and

$$\overline{F}_{\Phi}(ka,\tau) = \sum_{m=-\infty}^{+\infty}(-1)^{m+1}\frac{J_m(ka)}{H_m^{(2)}(ka)} \exp\left\{-\frac{i\tau}{1+i\tau}\left(\frac{m}{k\rho_0}\right)^2\right\}$$

$$(A.13)$$

$$\overline{F}_{\Psi}(ka,\tau) = \sum_{m=-\infty}^{+\infty}(-1)^m\frac{J_m'(ka)}{H_m^{(2)'}(ka)} \exp\left\{-\frac{i\tau}{1+i\tau}\left(\frac{m}{k\rho_0}\right)^2\right\}$$

54

Expanding the exponent in (A.12) into a power series in cotg γ_y and neglecting 6th and higher order terms we finally obtain

$$G_{E,r} = 4 \sqrt{\pi}^{-1} \sqrt{\frac{\varepsilon}{\mu}} k^2 v_0 \left(\frac{i\tau}{1+i\tau}\right)^{3/2} F_{E,r}(k u, \tau) \frac{1}{\sin^2\gamma_1 \sin^4\gamma_2 \, p(\gamma_1 \cdot \gamma_2)} \times$$

$$\times \exp\left\{-i 2 k d \left[1 - \frac{1}{2} \frac{\tau^2}{1+\tau^2} \cot g^2\gamma_1 - \frac{1}{4} \frac{\tau^2}{(1+\tau^2)^4} (4+5\tau^2 - 10\tau^4 - 3\tau^6)\cot g^2\gamma_1 \cdots \right]\right\} \times$$

(A.14)

$$\times \exp\left\{-(k \rho_0)^2 \left[\cot g^2\gamma_2 + \frac{1}{1+\tau^2} \cot g^2\gamma_1 - \frac{\tau^2}{(1+\tau^2)^4} (2+5\tau^2 + \tau^4)\cot g^4\gamma_1 \cdots \right]\right\}$$

APPENDIX B

ASYMPTOTIC EVALUATION OF RECIPROCITY INTEGRALS Q_θ AND Q_ϕ (Arbitrary Illumination)

Assuming that the wire is located in the far field region of the antenna, we evaluate expressions (30) for Q_θ and Q_ϕ asymptotically using the method of stationary phase. For large kd, the exponential function $\exp\{-ikd\,(\cos\alpha + \cos\alpha')\sin\beta\}$ varies rapidly with α, α', β, and all other terms in the integrands on the right-hand side of equations (30) can be regarded as slowly varying when compared to this function. Differentiation with regard to α, α', and β shows that the exponent has one saddle point within the range of integration* at

$$\alpha, \alpha' = 0 \ , \qquad \beta = 90°$$

Since kd is assumed to be very large, only the immediate neighborhood of this stationary point will contribute appreciably to the value of the integrals Q_θ and Q_ϕ. In this neighborhood, all terms of the integrands apart from the exponential function remain essentially constant; for the exponent, we use the second order approximation

$$ikd\,(\cos\alpha + \cos\alpha')\sin\beta \sim i2kd - ikd\left(\frac{\alpha^2 + \alpha'^2}{2} + \Delta\beta^2\right)$$

where $\Delta\beta = \beta - \pi/2$. Without sacrificing accuracy, the range of integration can be extended to $-\infty < \alpha, \alpha', \beta < +\infty$. Using the relation

$$\int_{-\infty}^{+\infty} e^{i\lambda u^2}\,du = \sqrt{\frac{i\pi}{\lambda}}$$

---

*On the boundary of the range of integration, the exponent has further saddle points at $\alpha, \alpha' = \pm\pi/2$, $\beta = 0$, π. These stationary points, however, do not yield an asymptotic contribution to Q_θ and Q_ϕ as the slowly varying part of the integrand at $\beta = 0$, π becomes zero.

we thus obtain for Q_ϕ and Q_ψ

$$Q_\phi = -16 \pi^{5/2} \sqrt{\frac{\varepsilon}{\mu}} \, k^2 \, \overline{F_\phi}(ka,0) \, \frac{e^{-i(2kd + \frac{\pi}{4})}}{(kd)^{3/2}} \, f^2(0,0)$$

$$(B.1)$$

$$Q_\psi = -16 \pi^{5/2} \sqrt{\frac{\varepsilon}{\mu}} \, k^2 \, F_\psi(ka,0) \, \frac{e^{-i(2kd + \frac{\pi}{4})}}{(kd)^{3/2}} \, g^2(0,0)$$

where $F_\phi(ka,0)$ and $F_\psi(ka,0)$ are given by equations (A.13) with $\tau = 0$.

DOCUMENT CONTROL DATA - R&D

(Security classification of title, body of abstract and indexing annotation must be entered when the overall report is classified)

1. ORIGINATING ACTIVITY *(Corporate author)*	2a. REPORT SECURITY CLASSIFICATION
U. S. Army Electronics Command Fort Monmouth, New Jersey 07703	UNCLASSIFIED
	2b. GROUP

3. REPORT TITLE

RADAR RESPONSE OF LONG WIRES

4. DESCRIPTIVE NOTES *(Type of report and inclusive dates)*
Technical Report

5. AUTHOR(S) *(Last name, first name, initial)*

F. Schwering

6. REPORT DATE	7a. TOTAL NO. OF PAGES	7b. NO. OF REFS
March 1970	57	17

8a. CONTRACT OR GRANT NO	9a. ORIGINATOR'S REPORT NUMBER(S)
b. PROJECT NO. 1T0 61102 B31A 01 45	ECOM-3246
c.	9b. OTHER REPORT NO(S) *(Any other numbers that may be assigned this report)*
d.	

10. AVAILABILITY/LIMITATION NOTICES
Distribution Statement No. 1: This document has been approved for public release and sale; its distribution is unlimited.

11. SUPPLEMENTARY NOTES	12. SPONSORING MILITARY ACTIVITY
	U. S. Army Electronics Command Fort Monmouth, New Jersey 07703 AMSEL-XL-L

13. ABSTRACT Scatter field and radar response of an infinitely long straight metallic wire are derived assuming that the wire is illuminated by an antenna radiating a Gaussian beam of narrow beam width. The scatter field has essentially the same distribution in any plane through the wire axis; it varies from plane to plane by only an amplitude factor. The radar response is at a maximum for vertical incidence - when the beam axis intersects the wire axis at right angles - and decreases exponentially with increasing inclination of the beam axis against this direction. No side lobes are obtained for Gaussian illumination, at least not in the interesting range of small angular deviations from vertical incidence where the radar response has a appreciable values. Two cases can be distinguished: (1) the wire crosses the Fresnel region of the antenna and (2) the wire is situated in the antenna far zone. In the former case, the theory is limited to wire radii not exceeding the beam radius at the antenna; in the latter case, arbitrary wire radii are admissible. If the wire is located in the far field region of the antenna, the expression derived for the radar response can be generalized so that it applies to any antenna characteristic. The generalized expression shows that a radar cross section can be assigned to the wire even though it has been assumed to be infinitely long; this radar cross section increases linearly with distance between antenna and wire.

14. KEY WORDS	LINK A		LINK B		LINK C	
	ROLE	WT	ROLE	WT	ROLE	WT
Scatter field of long metallic wire						
Radar response of long metallic wire						
Radar cross section of long metallic wire						
Long metallic wire with Gaussian illumination						
Wire crossing Fresnel region of Gaussian antenna						
Wire in far field region of Gaussian antenna						

INSTRUCTIONS

1. ORIGINATING ACTIVITY: Enter the name and address of the contractor, subcontractor, grantee, Department of Defense activity or other organization (corporate author) issuing the report.

2a. REPORT SECURITY CLASSIFICATION: Enter the overall security classification of the report. Indicate whether "Restricted Data" is included. Marking is to be in accordance with appropriate security regulations.

2b. GROUP: Automatic downgrading is specified in DoD Directive 5200.10 and Armed Forces Industrial Manual. Enter the group number. Also, when applicable, show that optional markings have been used for Group 3 and Group 4 as authorized.

3. REPORT TITLE: Enter the complete report title in all capital letters. Titles in all cases should be unclassified. If a meaningful title cannot be selected without classification, show title classification in all capitals in parenthesis immediately following the title.

4. DESCRIPTIVE NOTES: If appropriate, enter the type of report, e.g., interim, progress, summary, annual, or final. Give the inclusive dates when a specific reporting period is covered.

5. AUTHOR(S): Enter the name(s) of author(s) as shown on or in the report. Enter last name, first name, middle initial. If military, show rank and branch of service. The name of the principal author is an absolute minimum requirement.

6. REPORT DATE: Enter the date of the report as day, month, year, or month, year. If more than one date appears on the report, use date of publication.

7a. TOTAL NUMBER OF PAGES: The total page count should follow normal pagination procedures, i.e., enter the number of pages containing information.

7b. NUMBER OF REFERENCES: Enter the total number of references cited in the report.

8a. CONTRACT OR GRANT NUMBER: If appropriate, enter the applicable number of the contract or grant under which the report was written.

8b, 8c, & 8d. PROJECT NUMBER: Enter the appropriate military department identification, such as project number, subproject number, system numbers, task number, etc.

9a. ORIGINATOR'S REPORT NUMBER(S): Enter the official report number by which the document will be identified and controlled by the originating activity. This number must be unique to this report.

9b. OTHER REPORT NUMBER(S): If the report has been assigned any other report numbers (either by the originator or by the sponsor), also enter this number(s).

10. AVAILABILITY/LIMITATION NOTICES: Enter any limitations on further dissemination of the report, other than those imposed by security classification, using standard statements such as:

(1) "Qualified requesters may obtain copies of this report from DDC."

(2) "Foreign announcement and dissemination of this report by DDC is not authorized."

(3) "U. S. Government agencies may obtain copies of this report directly from DDC. Other qualified DDC users shall request through

_____."

(4) "U. S. military agencies may obtain copies of this report directly from DDC. Other qualified users shall request through

_____."

(5) "All distribution of this report is controlled. Qualified DDC users shall request through

_____."

If the report has been furnished to the Office of Technical Services, Department of Commerce, for sale to the public, indicate this fact and enter the price, if known.

11. SUPPLEMENTARY NOTES: Use for additional explanatory notes.

12. SPONSORING MILITARY ACTIVITY: Enter the name of the departmental project office or laboratory sponsoring (paying for) the research and development. Include address.

13. ABSTRACT: Enter an abstract giving a brief and factual summary of the document indicative of the report, even though it may also appear elsewhere in the body of the technical report. If additional space is required, a continuation sheet shall be attached.

It is highly desirable that the abstract of classified reports be unclassified. Each paragraph of the abstract shall end with an indication of the military security classification of the information in the paragraph, represented as (TS), (S), (C), or (U).

There is no limitation on the length of the abstract. However, the suggested length is from 150 to 225 words.

14. KEY WORDS: Key words are technically meaningful terms or short phrases that characterize a report and may be used as index entries for cataloging the report. Key words must be selected so that no security classification is required. Identifiers, such as equipment model designation, trade name, military project code name, geographic location, may be used as key words but will be followed by an indication of technical context. The assignment of links, rules, and weights is optional.

ESC-FM - 1227 - 70

(2)